



Flash flood-traffic interaction studies for the City of Ottawa

Keihan Kouroshejad

Department of Civil Engineering, McGill University, Montreal

December 2022

A thesis submitted to McGill University in partial fulfillment of the requirements of the degree of
Master of Engineering.

© Keihan Kouroshejad 2022

ABSTRACT

The main source of weather-related traffic delays in the summer is flash floods from short-duration, high-intensity precipitation events. This is particularly relevant for metropolitan areas because they have highly impervious surfaces like pavements and buildings. Future climate change is predicted to bring more of these flash flooding events. The impact of climate change, along with rapid urbanization, increasing the share of impervious areas, could worsen traffic disruption. This study investigates flash flood-traffic interactions for current and future climates for Ottawa, the capital city of Canada, by integrating ultra high-resolution (4 km) regional climate model (RCM) simulations with inundation modelling using PCSWMM, and exposure analysis based on transport network modelling. Flash floods associated with 100-year return levels of short-duration (i.e., 1-h, 3-h, and 5-h) precipitation events are considered in this study, with the projected changes to the return levels of precipitation estimated using two approaches: in the first approach projected changes are obtained directly from the RCM simulation, whereas in the second approach, these are obtained using temperature scaling (TS), which is recommended for practical applications.

Quantitative validation of the RCM-simulated precipitation characteristics, i.e. intensity-duration relations for selected return levels and their spatial variability, against gridded and station observations, along with qualitative validation of the hydrodynamic model simulated flash flood depths for past flooding, confirm suitability of the models in analyzing flash flood-related traffic disruptions. Results show projected increases in the 100-year return levels of 1-h, 3-h, and 5-h precipitation events to be 26, 16, and 30 % based on RCM and 55% based on TS over the study region for the future 2081-2100 period with respect to the 1991-2010 period, for the RCP8.5 scenario. This rise in the future precipitation suggests increases in the total length of blocked roads,

i.e., roads with flood depths higher than 30 cm, of approximately 28, 36, and 35 km based on TS and 26, 24, and 25 km based on GEM for the 1-h, 3-h, and 5-h events, respectively. This would translate to traffic disruption increases in the 60 to 77% range (33,000 to 38 person-hour delay) based on GEM and in the 57 to 59% range (28,000 to 29,000 person-hour delay) based on TS. By identifying the road links that are susceptible to flash flood-related traffic delays through a systematic combined analysis of flash flood-traffic interactions, this study provides crucial information in guiding the development of adaptation measures to increase resilience in the urban transportation network.

RESUME

La principale source de retards de la circulation liés aux conditions météorologiques en été est les crues soudaines causées par des événements de précipitations de courte durée et de forte intensité. Ceci est particulièrement pertinent pour les zones métropolitaines car elles ont des surfaces très imperméables comme les trottoirs et les bâtiments. On prévoit que le changement climatique futur apportera davantage de ces événements d'inondations soudaines. L'impact du changement climatique, ainsi que l'urbanisation rapide, augmentant la part des zones imperméables, pourraient aggraver les perturbations du trafic. Cette étude examine les interactions crue éclair-traffic pour les climats actuels et futurs d'Ottawa, la capitale du Canada, en intégrant des simulations de modèles climatiques régionaux (MRC) à ultra haute résolution (4 km) avec une modélisation des inondations à l'aide de PCSWMM et une analyse de l'exposition basée sur modélisation du réseau de transport. Les crues éclair associées à des niveaux de retour sur 100 ans d'événements de précipitations de courte durée (c. approches : dans la première approche, les changements projetés sont obtenus directement à partir de la simulation RCM, alors que dans la seconde approche, ceux-ci sont obtenus à l'aide de l'échelle de température (TS), ce qui est recommandé pour les applications pratiques.

La validation quantitative des caractéristiques des précipitations simulées par la MCR, c'est-à-dire les relations intensité-durée pour les niveaux de retour sélectionnés et leur variabilité spatiale, par rapport aux observations maillées et aux stations, ainsi que la validation qualitative des profondeurs de crue éclair simulées par le modèle hydrodynamique pour les inondations passées, confirment la pertinence du modèles pour analyser les perturbations du trafic liées aux crues éclair. Les résultats montrent que les augmentations projetées des niveaux de retour sur 100 ans des événements de précipitations de 1 h, 3 h et 5 h sont de 26, 16 et 30 % selon la RCM et de 55 %

selon la TS sur la région d'étude pour la future période 2081-2100 par rapport à la période 1991-2010, pour le scénario RCP8.5. Cette augmentation des précipitations futures suggère des augmentations de la longueur totale des routes bloquées, c'est-à-dire des routes avec des profondeurs d'inondation supérieures à 30 cm, d'environ 28, 36 et 35 km selon TS et 26, 24 et 25 km selon GEM pour les événements de 1 h, 3 h et 5 h, respectivement. Cela se traduirait par une augmentation des perturbations du trafic de l'ordre de 60 à 77 % (retard de 33 000 à 38 heures-personnes) selon le GEM et de 57 à 59 % (retard de 28 000 à 29 000 heures-personnes) selon le TS. En identifiant les liaisons routières susceptibles de subir des retards de circulation liés aux crues éclair grâce à une analyse combinée systématique des interactions crue éclair-circulation, cette étude fournit des informations cruciales pour guider l'élaboration de mesures d'adaptation visant à accroître la résilience du réseau de transport urbain.

ACKNOWLEDGEMENTS

I want to sincerely thank Prof. Laxmi Sushama, my supervisor, for all of her help during my master's program, including guidance, inspiration, motivation, and support. I would like to express my gratitude to my lab mates for our numerous fruitful discussions, their help with data preparation and extraction, and their insightful remarks and good advice that made my work much simpler. I would like to thank Compute Canada/Calcul Québec for providing the computational resources and Computational Hydraulics International (CHI) for providing PCSWMM software under CHI University Grant Program. I want to express my gratitude to my friends for their support, encouragement, and company. I appreciate the advice I received from the faculty and employees at McGill's civil engineering department. Finally, I want to express my gratitude to my family for their unwavering support. Without their assistance and ongoing support, none of this would have been possible.

CONTRIBUTION OF AUTHORS

This thesis has been written following the Graduate and Postdoctoral Studies requirements for a manuscript-based thesis. The main findings of the research undertaken by the author as part of his master's program are presented in a single manuscript. The author carried out the numerical analysis and wrote the manuscript under the supervision of Prof. Laxmi Sushama (supervisor). The publication detail is presented below:

- Kouroshnejad, K., Sushama, L. (2022). Flash flood-traffic interaction studies for the City of Ottawa (To be submitted to 'Water' journal).

TABLE OF CONTENTS

ABSTRACT	I
RESUME	III
ACKNOWLEDGEMENTS	V
CONTRIBUTION OF AUTHORS.....	VI
TABLE OF CONTENTS.....	VII
LIST OF FIGURES	IX
LIST OF TABLES.....	XII
CHAPTER 1 - INTRODUCTION.....	1
1.1 Background.....	1
1.2 Motivation.....	1
1.3 Research objectives.....	2
1.4 Thesis outline.....	3
CHAPTER 2 - LITERATURE REVIEW.....	5
2.1 Modelling of short-duration high-intensity precipitation events	5
2.2 Modelling of flood depths and velocities.....	10
2.3 Urban flood-traffic interactions	16
2.4 Urban traffic demand modelling.....	22
2.5 Knowledge gaps and conclusions	26

CHAPTER 3 – FLASH FLOOD-TRAFFIC INTERACTION STUDIES FOR THE CITY OF OTTAWA	28
ABSTRACT.....	28
3.1 Introduction.....	30
3.2 Models and Methods.....	33
3.2.1 Models.....	33
3.2.2 Methods.....	36
3.3 Results.....	38
3.3.1 Validation.....	38
3.3.2 Projected changes to PFF characteristics	39
3.3.3 Traffic disruption	42
3.4 Summary and conclusion.....	43
CHAPTER 4 - DISCUSSION	57
4.1 Assumptions, models, and methods.....	57
4.2 Preliminary exploration of added value using sub-km scale climate modelling	59
CHAPTER 5 - CONCLUSIONS AND RECOMMENDATIONS.....	63
REFERENCES	67

LIST OF FIGURES

Figure 2.1 Joint probability distribution of rain spell duration vs peak rainfall exceeding 0.1 mm/h, for (a) radar and model differences, (b),(e) 12 km - radar, (c),(f) 1.5 km - radar, and (d) 1.5 km - 12 km (Kendon et al., 2012).....	7
Figure 2.2 Biases in GEM simulations at 50 km (GEM50; top row) and 4 km (GEM4; bottom row) resolutions compared to DAYMET for summer average precipitation (%) and yearly and summer averages of maximum 2- m air temperature (°C) over the period 1991–2010 (Teufel and Sushama, 2022).....	8
Figure 2.3 The rainfall intensity of the 10-year event at 17 sites, for the 1991–2010 period, for durations ranging from 1 to 24 h, from observations (black lines), GEM4-ERA5 (dark blue lines) and GEM50-ERA (light blue lines) (Teufel and Sushama, 2022).....	8
Figure. 2.4 Projected changes to 2-yr return levels of 15-min (left), 1-h (center), and 4-h (right) rainfall for 2021–2040 with respect to 1991-2010 (Teufel and Sushama, 2022).....	9
Figure. 2.5 Validation of PCSWMM at two stations (Coulombe et al., 2022).....	12
Figure 2.6 Saint-Régis River Hydrographs for various adaptation strategies for a 25-year 3-h under current and future climate (Coulombe et al., 2022).....	12
Figure 2.7 Rolland-Therrien combined sewer catchment (Gooré Bi et al., 2015).....	13
Figure 2.8 Computed vs. observed maximum flows for eight rainfall-radar scenarios.....	15
Figure 2.9 Urban flood hazard map (Manchikatla and Umamahesh, 2022).....	16
Figure 2.10 Framework to evaluate the PFF-induced traffic disruption (Li et al., 2018).....	20
Figure 2.11 Disruption function (Pregnoiato, 2016).....	20
Figure 2.12 The framework to assess pluvial flood-induced disruption to the road network used in Pregnoiato et al. (2017).....	21

Figure 2.13 The four-stage transport model (Ortúzar and Willumsen, 2011).	23
Figure 3.1 (a) GEM experimental domain at 10 km (red) and 4 km (blue) resolutions, with every 25 th and 20 th gridlines, respectively, shown. (b) The road network and (c) drainage networks for the study domain consisting of eight inner wards of the City of Ottawa (shown in pink).	46
Figure 3.2 (a) Mean summer (June–August) precipitation from Daymet (left panel) for the 1991–2010 period, and GEM_ERA5 (center panel) and GEM_CanESM2 (right panel) biases. (b) Observed, GEM_ERA5, and GEM_CanESM2 simulated intensity-duration relations for 6 stations around the study area.	47
Figure 3.3 (a) The July 1, 2017 observed and GEM_ERA5 simulated precipitation event at OTTAWA CDA RCS. (b) PCSWMM simulated maximum flood depth for the event and (c) Digital Elevation Model at 5 m resolution.....	48
Figure 3.4 Design storms corresponding to 100-year return levels of 1-h, 3-h, and 5-h precipitation events for current (TSC1, TSC2, TSC3) and future climates (TSF1, TSF2, TSF3) at OTTAWA CDA RCS station; Future return levels are estimated using the temperature scaling approach.....	49
Figure 3.5 Max depth (top), total runoff depth (middle) and sewer max flow/capacity (bottom) for current climate (left column), and their projected changes (right column) for the 100-year return levels of 1-h precipitation for the temperature scaling approach.	50
Figure 3.6 Max depth (top), total runoff depth (middle) and sewer max flow/capacity (bottom) for current climate (left column), and their projected changes (right column) for the 100-year return levels of 3-h precipitation for the temperature scaling approach.	51

Figure 3.7 Max depth (top), total runoff depth (middle) and sewer max flow/capacity (bottom) for current climate (left column), and their projected changes (right column) for the 100-year return levels of 5-h precipitation for the temperature scaling approach. 52

Figure 3.8 Differences in maximum flood depths for the two approaches (GEM-based and temperature scaling-based) for current (left) and future (right) climates for 100-year return levels of (a) 1-h (top), (b) 3-h (center), and (c) 5-h (bottom) precipitation. 53

Figure 3.9 Percentage of the road network corresponding to various flood depth bins, for current (shaded bars) and future (hatched bars) climates, for 1-h (blue; C1h, F1h), 3-h (red; C3h, F3h) and 5-h (green; C5h, F5h) precipitation events for the TS (dark grey background) and GEM (light grey background) based approaches. 54

Figure 3.10 Speed reduction (in percentage) for 100-year 1-h (first column), 3-h (second column), and 5-h (third column) precipitation events for current (top) and future (bottom) climates for the (a) TS-based and (b) GEM-based approaches. 55

Figure 4.1 Projected changes to 100-year 1-, 3-, and 5-h precipitation using GEM and TS. 59

Figure 4.2 2017 July 1 event precipitation from GEM-ERA5 and GEM100-ERA5 simulations. 60

Figure 4.3 Total precipitation associated with the July 1, 2017 event from GEM_ERA5 (left) and GEM100_ERA5 (right) simulations. 61

Figure 4.4 Max flood depth simulated using rainfall data from (a) GEM_ERA5, (b) GEM100_ERA5. 62

LIST OF TABLES

Table 2.1 Comparison of VD and Q_CSO in current (2013) and future (2050) (Gooré Bi et al., 2015).	14
Table 2.2 Urban flood hazard index for urban areas (Manchikatla and Umamahesh, 2022).	16
Table 2.3 The statistical length of road network disruption (the total length is 43.2 km) (Yin et al., 2016).	19
Table 2.4 Total Person Hour for the 10- and 5-year events (Pregolato et al., 2017, (modified)).	21
Table 3.1 PHD for current and future climates; TS1 (G1), TS3 (G3), TS5 (G5) correspond to temperature scaling-based (GEM-based) approach for 1-h, 3-h and 5-h durations.....	56

CHAPTER 1 - INTRODUCTION

1.1 Background

Pluvial flash floods caused by high-intensity, short-duration precipitation events in urban regions can adversely impact engineering systems, e.g. those related to transportation. Such events can disrupt the road network in two ways: through infrastructure damages, that can lead to temporary failure of the system, or through traffic disruptions associated with flooded road links. The latter could lead to complete closure of flooded links at high flood depths and velocities or reduction in traffic flow speed. The reduced road network operations and efficiency during pluvial flash flooding can thus lead to significant delays in urban trips.

Due to the higher water holding capacity of the atmosphere at higher temperatures, such short-duration high-intensity precipitation events are expected to become more frequent and more intense in a future warmer climate, according to the IPCC (2013). This would imply severe adverse effects on the operation of the road network. To enhance the climate resiliency of the road network through the development and application of adaptation strategies, information on projected changes to such events at engineering scales, and transportation behavior under such scenarios are required.

1.2 Motivation

The transportation networks in urban areas could be severely disrupted by pluvial flash floods. This is a major issue as the road network needs to operate efficiently under all circumstances. An increase in the intensity and frequency of such events, as projected by the global climate models and which has already been witnessed in recent years in many parts around the world, including

Canada, elevates the vulnerability of the transportation network. As a result, pluvial flash flood-related traffic disruption has been gaining attention recently, although the literature lacks such studies for Canada.

In order to understand flash-flood traffic interactions in urban regions, an integrated framework comprising ultra-high resolution climate models that can generate climate change information at engineering scales, hydrodynamic models capable of simulating flood dynamics, and traffic models that capture traffic behavior, are required. With the rapid advances in the area of high-performance computing, it has now become possible to undertake climate change simulations at ultra-high resolutions, mostly in the 4 km to 2.5 km range. This will help in capturing the spatial and temporal variability at unprecedented scales, which when one-way coupled with the hydrodynamic flood and transport models can provide critical information, particularly related to hot spots of likely traffic disruptions, that can guide adaptation and traffic planning.

Therefore, the main goal of this study is to evaluate flash flood-induced traffic disruptions to the Ottawa road network in current and future climates, for an extreme Greenhouse Gas emission scenario. The results of this research will form the basis for additional studies, while also providing critical information regarding changing precipitation, flash-flood and traffic flow/disruption characteristics for the City of Ottawa, which can inform city officials and planners in their effort to enhance the climate resiliency of the urban transport network.

1.3 Research objectives

The main objective of this study is to evaluate the impacts of flash floods on road traffic for the city of Ottawa for current and future climates using the Global Environmental Multiscale (GEM)

regional climate model, PCSWMM integrated 1d-2d hydrodynamic model, and a GIS-based transport model. More specifically, this study:

- Conducts a literature review on the impact of climate change on intense precipitation and associated floods and their interactions with the transport network, particularly road traffic.
- Validates, quantitatively and qualitatively, the climate and hydrodynamic models used in this study.
- Estimates projected changes to 100-year return levels of short duration (1-h, 3-h, and 5-h) precipitation events based on two different approaches: GEM-based and temperature scaling-based approaches.
- Assesses projected changes to the pluvial flash flood-induced traffic disruptions in terms of person-hour delay.
- Draws conclusions on the impact of pluvial flash floods on travel time in current and future climates in light of the two approaches considered, while identifying/recommending future improvements/studies that can increase the robustness of the results of this study.

1.4 Thesis outline

The thesis is divided into four chapters: Chapter 1 provides a broad overview of the background, motivation for conducting the study, and objectives. Chapter 2 reviews literature pertinent to this study: modelling of short-duration high-intensity precipitation events, modelling of flood depth and velocities and transport modelling. Chapter 3 presents the main results of this study, i.e., impact of climate change on pluvial flash flood-induced traffic disruption for the city of Ottawa, which is presented in the form of a journal article, following the article-based thesis format.

Chapter 4 provides additional discussions and lastly, Chapter 5 summarizes the findings, offers ideas for additional pertinent research, and discusses limitations of this study.

CHAPTER 2 - LITERATURE REVIEW

The combined impacts of climate change and rapid urbanization can lead to severe impacts of pluvial flooding in urban areas, which could damage or disrupt urban systems. Among urban infrastructure, road networks, which are critical for moving goods and people, can be impacted by Pluvial Flash Floods (PFFs) in two ways: it can cause traffic disruptions and can also impact the structural integrity of the road infrastructure. Understanding the evolving characteristics of pluvial floods is important for developing adaptation strategies for the road network, which is the focus of this study. This chapter reviews advances in related topics such as modelling pluvial floods, i.e., modelling of high-intensity short-duration precipitation and hydrodynamic modelling, and their traffic interactions.

2.1 Modelling of short-duration high-intensity precipitation events

Global climate models (GCMs) are the most comprehensive tools used to study climate and climate change. Due to the complexity of these models, they are usually run at coarse resolutions in the 110–550 km range. GCMs are downscaled statistically or dynamically using statistical methods or regional climate models (RCMs) to higher resolutions. RCM simulations, generally in the 10 to 20 km range, are usually performed over a specific domain with lateral boundary conditions coming from GCMs. In order to assess the biases associated with GCM boundary data in these simulations, it is compared with a simulation performed using the deemed unbiased boundary conditions of global reanalysis, such as ERA5 (Giorgi, 2019; Rummukainen, 2010). Also, comparing reanalysis-driven RCM simulation outputs with observed data could yield model errors, which is generally referred to as performance errors.

Though the horizontal resolution of the GCMs and RCMs considered is fine enough to simulate large-scale weather and climate systems, it is insufficiently fine to describe many important

processes (such as convective cloud systems) that rarely extend beyond a few kilometres (Sushama et al., 2021). At coarse grid resolutions the average effects of convective clouds and other small-scale processes within a grid box are approximated using simplified formulae known as 'parameterizations'. These approximations are the main source of errors and uncertainties in climate simulations (Palmer, 2014). For instance, climate models with convection parameterization, which aims to describe the average properties of convection over a model grid box, leads to deficiencies in the diurnal cycle of convection, precipitation occurrence, variability and extremes (Prein et al., 2015). This implies that our confidence in model projections of changes in local precipitation extremes and other phenomena, which are crucial in local planning and decision-making processes, is limited because of deficiencies in the representation of key small-scale processes. Therefore, higher resolution climate modelling is needed to have a climate simulation that accounts for important small-scale processes. Ultra-high resolution simulation made by decreasing the size of grid cells of the climate model to kilometre scale would allow major convective cloud systems to be resolved explicitly and consequently termed as convection-permitting climate model (CPM) simulation or ultra-high resolution simulations. Such simulations thus generate climate information at the spatial and temporal scales required for many engineering applications.

Kendon et al. (2012) assessed the differences in the performance of a 12km- RCM and a 1.5 km CPM in simulating rainfall over the united kingdom. Their results show that CPM better represents the spatio-temporal characteristics of rainfall events. Moreover, they showed that heavy rainfalls are better captured by the CPM compared to the RCM on the basis of radar data (Fig. 2.1).

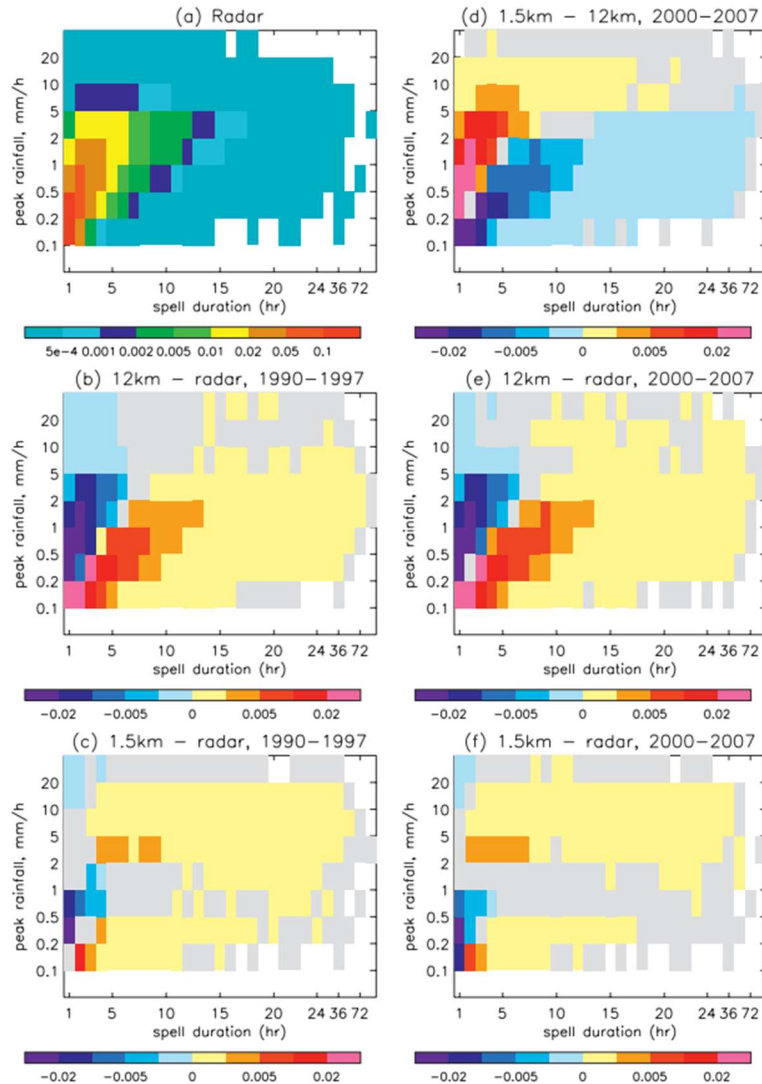


Figure 2.1 Joint probability distribution of rain spell duration vs peak rainfall exceeding 0.1 mm/h, for (a) radar and model differences, (b),(e) 12 km - radar, (c),(f) 1.5 km - radar, and (d) 1.5 km - 12 km (Kendon et al., 2012).

Similarly, Teufel and Sushama (2022) performed RCM (50 km) and CPM (4 km) simulations over a domain covering eastern and central Canadian Arctic for the current (1991-2010) period and assessed the added value of the higher resolution in the CPM simulation. Significant improvements were noted, both for mean (Fig. 2.2) and extreme (Fig. 2.3) precipitation. The intensity-duration

relations, particularly for shorter durations, for 100-year return levels, at 17 sites, simulated at 4 km resolution showed clear improvements compared to the 50 km resolution simulation.

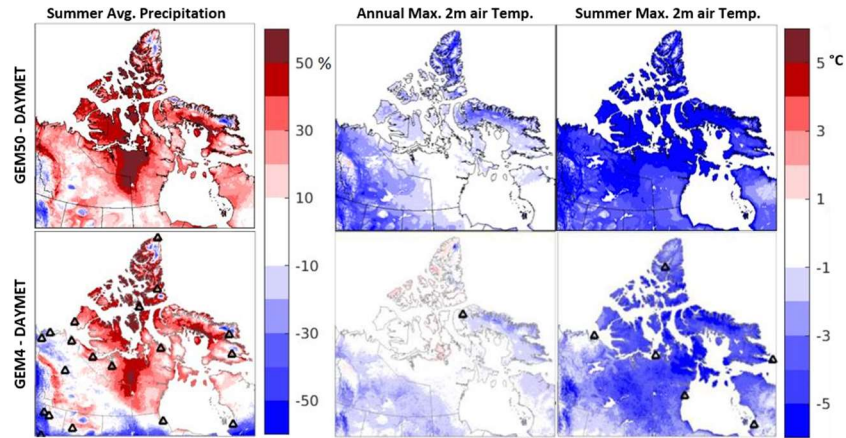


Figure 2.2 Biases in GEM simulations at 50 km (GEM50; top row) and 4 km (GEM4; bottom row) resolutions compared to DAYMET for summer average precipitation (%) and yearly and summer averages of maximum 2- m air temperature ($^{\circ}\text{C}$) over the period 1991–2010 (Teufel and Sushama, 2022).

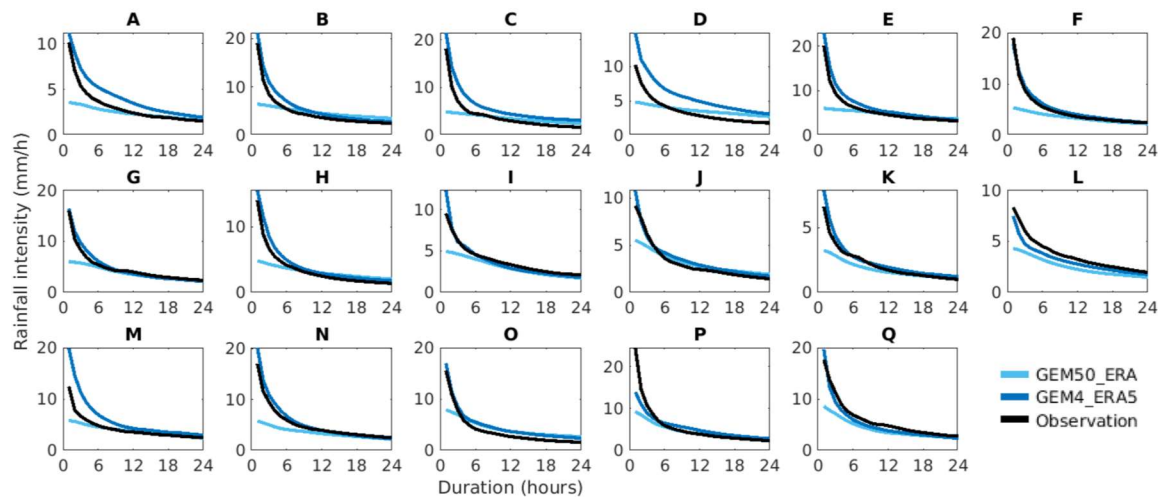


Figure 2.3 The rainfall intensity of the 10-year event at 17 sites, for the 1991–2010 period, for durations ranging from 1 to 24 h, from observations (black lines), GEM4-ERA5 (dark blue lines) and GEM50-ERA5 (light blue lines) (Teufel and Sushama, 2022).

Moreover, climate change simulations were also performed by Teufel and Sushama (2022) at 4 km resolution, for the RCP 8.5, driven by the Canadian Earth System (CanESM2) at the lateral

boundaries; their results suggest projected increases in the 2-year return levels, of 15 min to 4 hour duration precipitation events, for most of the studied region, with increases higher than 50% in some regions, for the future 2021-2040 period with respect to the current 1991-2010 period (Fig. 2.4)

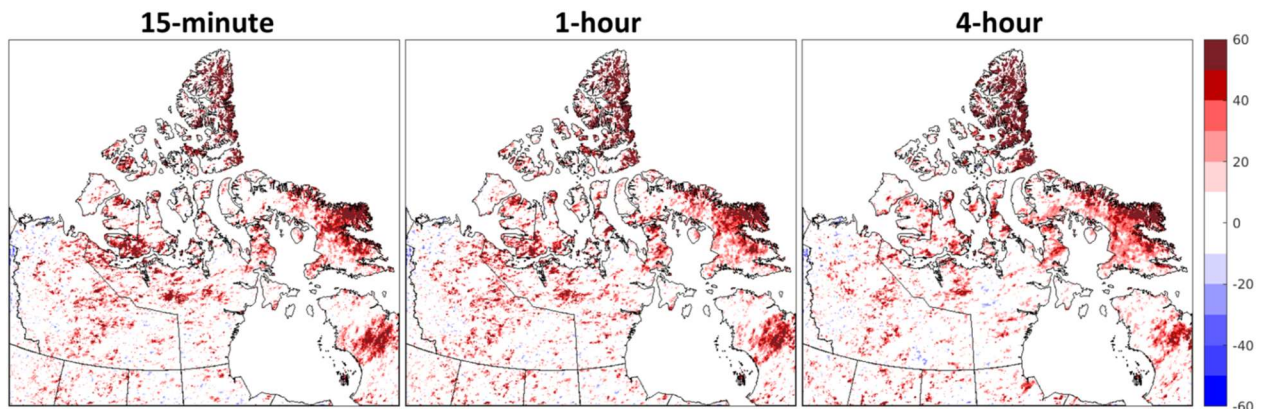


Figure. 2.4 Projected changes to 2-yr return levels of 15-min (left), 1-h (center), and 4-h (right) rainfall for 2021–2040 with respect to 1991-2010 (Teufel and Sushama, 2022).

Climate simulations at ultra-high resolution are computationally expensive, and therefore, other methods based on temperature-scaling have been proposed to estimate future changes to precipitation extremes. This approach is supported by the following: Firstly, it is widely known and confirmed in many studies that the underlying causes for the increase in the intensity and frequency of future precipitation are attributable to the increased moisture holding capacity of the atmosphere at higher temperatures (Trenberth, 2011; Held and Soden, 2006). Fowler and Wilby (2010) also demonstrated this over a region comprising the United Kingdom. Secondly, as extreme precipitation events do not occur relatively often, the confidence in their projections and analysis is not as accurate as temperature (Warner et al., 2012). Therefore, analyzing temperature and warming trends is a viable and less costly approach to examining future precipitation patterns.

The temperature scaling (TS) method, recommended by Environment and Climate Change Canada, the Canadian Highway Bridge Design Code, and the National Building Code of Canada (CSA PLUS 4013), approximates the relationship between the current and future precipitation return levels by considering long term changes of temperature as:

$$R_F = R_C \times 1.07^{\Delta T} \quad (1)$$

where R_F is the future return level, R_C is the current return level, and ΔT is the projected temperature change between the current and future epochs.

2.2 Modelling of flood depths and velocities

Flood modelling approaches include, one-dimensional overland (1D) and sewer (1D-S), two-dimensional overland (2D), integrated 1D-1D and 1D-2D, and rapid flood spreading (RFS). When choosing the model type, several things need to be considered. These include the processes that need to be represented in the model for the results to be accurate, how the final results will be used, and the available computational resources.

The integrated 1D-2D is the most advanced approach in flood modelling. In this approach, the flood plain is characterized by the overland 2-D mesh connected to the 1-D drainage network. The 1D and 2D systems interact at catch basins. This approach is generally used in complex urban settings where the highest accuracy of flood characteristics is expected. The main outputs from 1D-2D integrated models are flow characteristics such as flood water depth and velocity, flood extent, and hotspots in the drainage system. However, accurate results require high computational resources and run-time (Bamford et al., 2008; Leandro et al., 2009) and entail more precise input data. These make the integrated 1D–2D modelling approach inefficient for real-time applications.

To lower the cost of computing, it may be necessary to use DEM data with a lower resolution or use larger grid cells and less detail inside the model.

A number of flood modelling software packages exist, such as HEC-RAS, CityCAT, and PCSWMM. The hydrodynamic model PCSWMM, developed by Canada Computational Hydraulics International (CHI), is based on EPA SWMM. It combines GIS engines with SWMM and is capable of hydrologic and hydraulic modelling. This software has been used in various studies for applications ranging from rainfall-runoff modelling, urban drainage modelling, low-impact development assessments, and integrated 1D-2D flood modelling, in different countries, showing the suitability of the model for application in different climatic regions. Examples of studies that applied PCSWMM for flood modelling in Canada are discussed below.

Coulombe et al. (2022) used PCSWMM to simulate flooding in Saint-Isidore municipality from the Saint-Régis River located in Quebec, Canada, in order to develop adaptation strategies. The rainfall considered in this study is the 25-year 3-h Chicago design storm which is augmented by 18% to account for the impact of climate change. PCSWMM is first calibrated and validated based on historical water level data at two stations, as shown in Fig 2.5, and is run for various combinations of adaptation strategies in the current and future climate.

Figure 2.6 (from Coulombe et al. (2022)) demonstrates the efficiency of employing each combination of adaptation strategies in lowering peak flows at the Saint-Regis river outlet. It shows that the addition of each adaptation strategy may yield improvements, while a combination of them leads to the highest efficacy in reducing the flow peak to as low as 2.5 and $3.2 \frac{m^3}{s}$ for current and future climates, respectively.

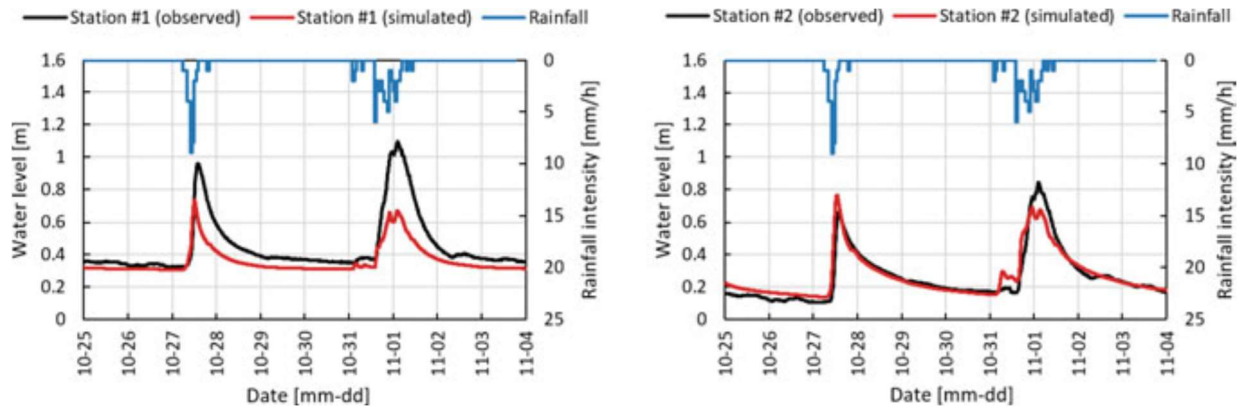


Figure 2.5 Validation of PCSWMM at two stations (Coulombe et al., 2022).

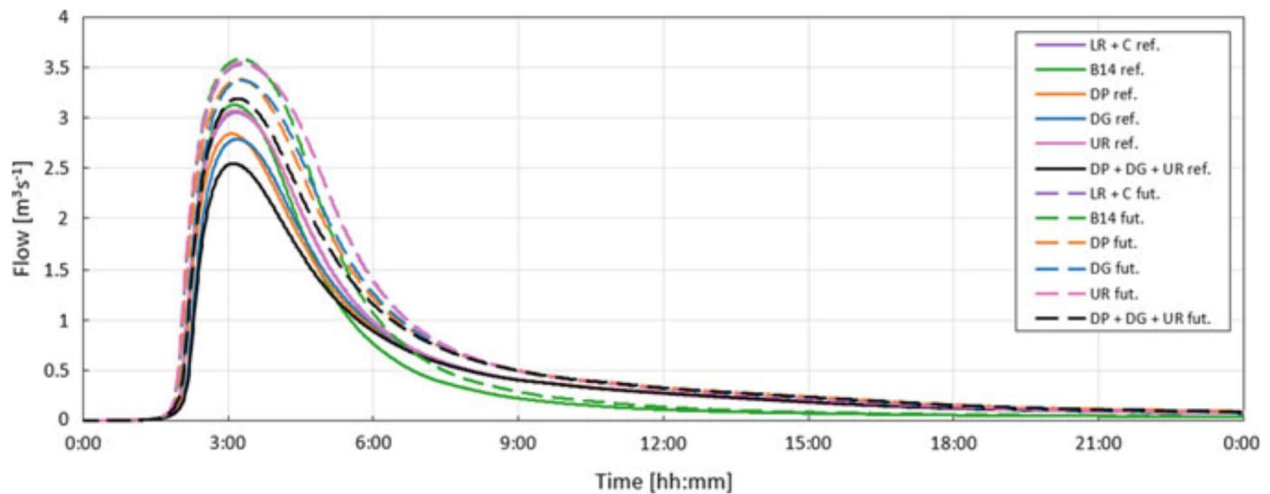


Figure 2.6 Saint-Régis River Hydrographs for various adaptation strategies for a 25-year 3-h under current and future climate (Coulombe et al., 2022).

Gooré Bi et al. (2015) assessed the impact of the increase in extreme precipitation events due to climate change on the risk of the Rolland-Therrien combined sewer system overflow into the ST.lawrence river in Longueuil, Canada (Fig. 2.7). In this study, PCSWMM is applied to simulate projected changes to the combined sewer system overflow in the future (2050) with respect to current (2013) conditions, where VD (volume discharge) and Q_{CSO} (peak combined sewer overflow) are considered to quantify the magnitude of system overflow. PCSWMM is first

calibrated using historical data from the eight events in the summer of 2013. Subsequently, the model is run considering a 20% increase in the total rainfall due to climate change for 2050 for similar events.

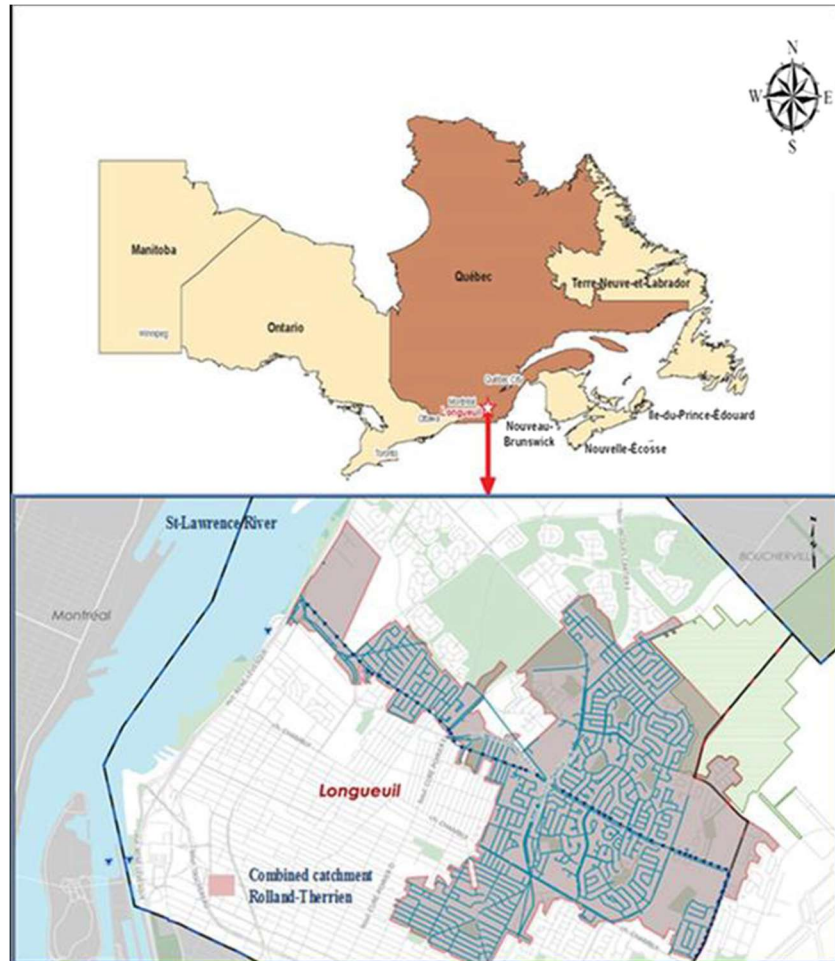


Figure 2.7 Rolland-Therrien combined sewer catchment (Gooré Bi et al., 2015).

Their results show projected changes to the VD and Q_{CSO} in the range of 15 to 500 and 13 to 148%, respectively; nonlinearity of the relation between overflow discharge and rainfall intensity; and the need to consider improvement to the combined sewer system due to the impact of climate change (table 2.1).

Table 2.1 Comparison of VD and Q_{CSO} in current (2013) and future (2050) (Gooré Bi et al., 2015).

Event	Reference climate (2013)			Future climate (2050)			Increase (2050/2013) in %			Ratio (2050/2013)		
	RI (mm/h)	VD (m ³)	Q_{CSO} (m ³ /s)	RI (mm/h)	VD (m ³)	Q_{CSO} (m ³ /s)	RI	VD	Q_{CSO}	RI	VD	Q_{CSO}
July 17	62.4	23,100	7.90	74.9	32,400	9.54	20	40	21	1.2	1.4	1.2
July 19	27.6	12,300	3.84	33.1	28,400	6.31	20	132	64	1.2	2.3	1.6
August 1	16.8	8300	2.67	20.2	16,100	4.40	20	95	65	1.2	1.9	1.6
September 12	21.6	15,800	3.12	25.9	24,100	3.54	20	52	13	1.2	1.5	1.1
October 6	3.6	305	0.21	4.30	1800	0.52	20	500	148	1.2	6.0	2.5
October 7	27.6	22,800	3.08	33.1	26,300	3.53	20	15	14	1.2	1.2	1.1
Minimum	3.60	305	0.21	4.30	1800	0.52	20	15	13	1.2	1.2	1.1
Maximum	62.4	23,100	7.90	74.9	32,400	9.54	20	500	148	1.2	6.0	2.5
Mean	25.0	13,800	3.5	30.0	21,500	4.64	20.0	139	54	1.2	2.4	1.5

CSO combined sewer overflow, *RI* rainfall intensity maximal in 5 min, *VD* volume discharged, Q_{CSO} CSO peak flow

PCSWMM could be applied in real-time flood forecasting applications where precipitation information is derived from the real-time radar providing high-resolution spatio-temporal data. Toronto and Region Conservation Authority and Computational Hydraulics International used PCSWMM to develop a real-time flood forecasting system for the 360,000-ha Don river to simulate hydrodynamic properties of the catchment and flood flow in real-time (James et al.). The catchment is discretized into 70 sub-catchments, the characteristics of which are derived from the land use and soil information, and 225km of natural canals are incorporated into the hydraulic simulations. Real-time precipitation data are derived from the Next Generation Radar (NEXTRAD) level II. The hydrodynamic model is calibrated based on ten extreme precipitation events using eight different methods to bias-correct the rain gauge radar data. Results show the highest agreement between the Max flow based on observations and the Digital hybrid scan reflectivity (DHSR) radar data within 20% of the observed max flow (Fig. 2.8). This method is employed in the current real-time flood forecasting system by Toronto and Region Conservation Authority.

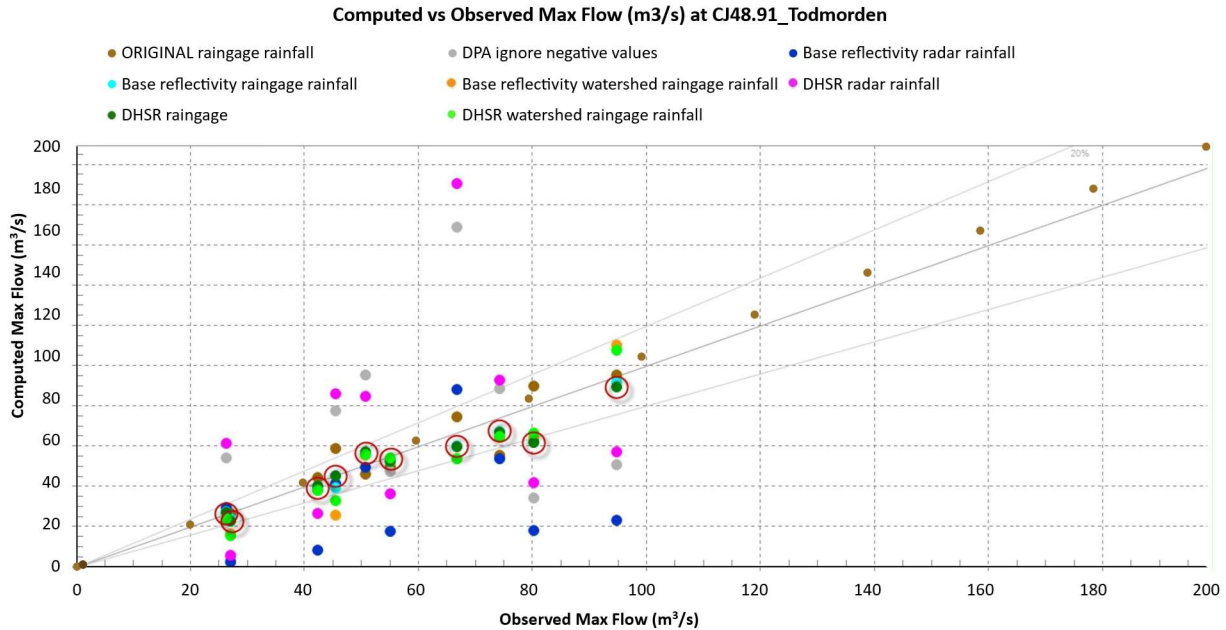


Figure 2.8 Computed vs. observed maximum flows for eight rainfall-radar scenarios.

PCSWMM has been widely applied in many countries for various applications. For example, Ahiablame and Shakya (2016) employed PCSWMM in order to evaluate the flood reduction effects of low impact development strategies in central Illinois. Akhter and Hewa (2016) used PCSWMM to investigate the impacts of land use change on the Mypogna catchment response in Australia.

Manchikatla and Umamahesh (2022) assessed flood hazards for the two most flood-prone zones of an Indian city (Hyderabad) by performing a 1D-2D integrated flood modelling using PCSWMM for a historical event in October 2020. PCSWMM is used to delineate sub-catchments based on DEM and to simulate the drainage network and overland flow in 1d and 2d, respectively. The validation of the model is performed by comparing the simulated water depth with those from social media references and station observations. In this study, flood risk is defined based on the

product of the depth and velocity of floodwater, denoted as the urban flood hazard (UFH) index (Table. 2.2).

Table 2.2 Urban flood hazard index for urban areas (Manchikatla and Umamahesh, 2022).

UFH index	Depth of inundation, D (m)	Velocity of moving stormwater, V (m/s)	Hazard classification limit $D \cdot V$ (m^2/s)	Description
UFH1	$0 \leq D \leq 0.3$	≤ 1.5	≤ 0.3	Safe for vehicles, public and settlements but problem to traffic
UFH2	$0.3 \leq D \leq 0.5$	≤ 1.5	≤ 0.6	Unsafe for vehicles and children
UFH3	$0.5 \leq D \leq 1.0$	≤ 1.5	≤ 1.0	Unsafe for all vehicles and public
UFH4	$D > 1.0$	> 1.5	> 1.0	Unsafe for all vehicles, public and all types of settlements

Figure 2.9 (from Manchikatla and Umamahesh (2022)) shows the hazard map for one of the zones based on UHI, showing extreme hazards mostly in the northern parts and in locations such as Sai Nagar and Kakatiya Colony.

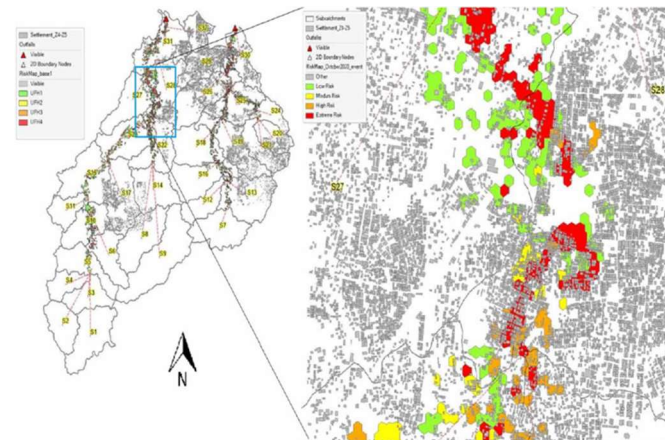


Figure 2.9 Urban flood hazard map (Manchikatla and Umamahesh, 2022).

2.3 Urban flood-traffic interactions

PFFs can ravage the infrastructure and disrupt urban systems (Spekkers et al., 2011). Certain properties of an urban environment could amplify the impacts of pluvial floods. For example, the

high proportion of paved surfaces that act as impervious surfaces results in a huge reduction in the ability of the underground soil to drain the running water (Mote et al., 2007; Shepherd et al., 2002). Also, more urbanization worsens flood risk by exposing more people and infrastructure to flooding (Barredo, 2009; Mitchell, 2003). Furthermore, the conditions of urban infrastructures, such as drainage systems, are important factors that can dilute or worsen urban flood consequences. For instance, in Canada, a large proportion of the drainage network facilities, worth 10 billion dollars, are in poor condition (Canadian Infrastructure Report Card, 2016). This could aggravate the flooding consequences.

A unanimously agreed definition of flood risk is the probable consequences, i.e., the multiplication of the probability of a hazard and the consequences incurred. In this manner, the exposure and vulnerability of assets are the two elements that determine the consequence of an event. For the flood-related damage estimation of structures, certain damage curves could be utilized, relating the depth or velocity of flood water to the resulting damage. Such functions are derived from the observed data of historical events or surveys (Penning-Rowsell et al., 2014). Several studies have assessed the impact of floods on the physical damage to infrastructures (e.g., Dutta et al., 2003; Hammond et al., 2015; Jonkman et al., 2008a, 2008b; Kellermann et al., 2016; Scawthorn et al., 2006). Jonkman and Kelman (2005) developed a function relating the death rate to the flood depth.

PFF impacts on the transport network can be classified as direct or indirect (Brown and Dawson, 2016; Hammond et al., 2015). The former corresponds to the incurred damage to the transport infrastructure, which could lead to partial or complete system failure and even casualties. Arkell and Darch (2006) and Hooper et al. (2014) have shown that many flood-related deaths are related

to transportation. PFFs are deemed to be the principal cause of disruption to the road network (DfT, 2014a), and some related studies are presented below.

Traffic interactions

The impact of pluvial flash floods on travel delays in the road network has been getting more attention in recent years, although thorough research is still lacking. Research has been undertaken in order to assess the impact of flooding on the safety and operation of road links (Andrey et al., 2003; Eisenberg, 2004); however, these are not capable of performing a citywide analysis of traffic delays.

A number of studies applied a disaggregate transport model to assess the impact of flooding on the road network (Chen, 2008; Su et al., 2016; Park & Kwak, 2011). It should be noted that researching the impacts of flooding on the disruptions in a transport system requires a citywide analysis with a certain level of aggregation. A micro-scale approach may be considered in cases where the objective is to evaluate a small region's serviceability or limit states or the role of specific mechanisms in the outcomes, such as performing a sensitivity analysis.

Yin et al. (2016) integrated flood inundation with traffic demand modelling for the city center of Shanghai and considered the road links with flood depth higher than 30 cm (direct impact) and the links connected to them (indirect impact) to be fully blocked. They employed spatially constant precipitation data derived from the Chicago design storm for 5-, 10-, 20-, 50-, and 100-year events.

Table 2.3 summarizes the results of this study. The total disruption increases for the less probable events and the disruption duration increases as the events' intensity increases. Also, the total length of closed links under a 100-year event is double the 5-year event and the total length of the road

network PFF directly impacts is approximately 21 km, corresponding to half of the road network. Furthermore, they showed that the relation between the PFF magnitude and traffic disruption is not linear.

Table 2.3 The statistical length of road network disruption (the total length is 43.2 km) (Yin et al., 2016).

Duration (h)	Total (indirect disruption) length (km)				
	5-year	10-year	20-year	50-year	100-year
0–0.5	0.65(/)	0.83(/)	0.39(0.14)	0.43(0.14)	0.18(/)
0.5–1	1.60(/)	0.95(/)	1.09(/)	5.11(3.94)	1.17(0.31)
1–1.5	0.24(/)	1.48(/)	1.52(/)	0.87(/)	0.94(0.05)
1.5–2	2.22(0.14)	0.71(/)	1.66(0.16)	0.71(/)	4.34(2.70)
2–2.5	0.91(/)	0.67(/)	1.11(/)	1.30(0.19)	0.69(/)
2.5–3	1.54(/)	1.87(/)	1.96(0.10)	2.08(/)	1.20(0.12)
3–3.5	2.84(/)	5.24(/)	5.82(0.11)	7.58(0.17)	7.37(0.11)
3.5–4	5.96(/)	7.78(0.08)	12.31(/)	16.44(/)	20.81(/)
Total	15.95 (0.14)	19.52 (0.08)	25.85 (0.51)	34.52 (4.44)	36.68 (3.29)

Li et al. (2018) used a similar approach in the city center of Shanghai to assess the traffic disruption and delays in pluvial flash flood conditions under 10, 20, 50, and 100-year events (Fig. 2.10). They used a simplified assumption for considering road links as entirely blocked or operational, with the closure and opening times of road links defined based on a flood depth threshold of 30 cm. The traffic model is updated every 5 seconds in order to identify new flood depths on the road network. Their results show that the travel delays could be 0.5 to 8 times greater than travel times in a non-flood condition. The absence of factors such as the dynamic modelling of the drainage network and considering the spatial variations of precipitation led to deficiencies in this study.

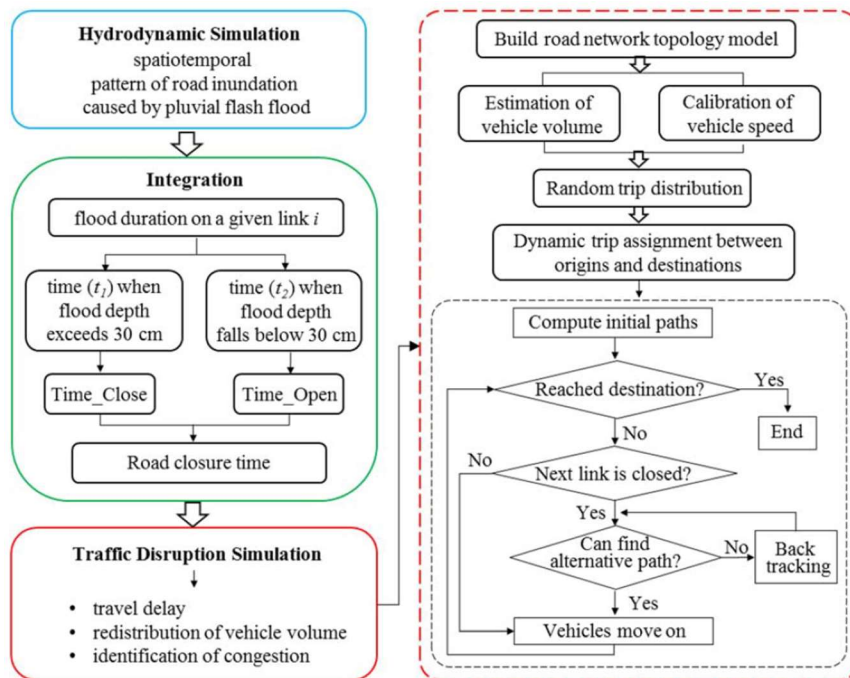


Figure 2.10 Framework to evaluate the PFF-induced traffic disruption (Li et al., 2018).

Pregolato et al. (2016) used reported and observed data from past floods as well as video analysis to make a depth-disruption function (Fig. 2.11) that links the safe speed to the depth of flood water on the roads. This moves beyond the crude assumption that no traffic disruption (i.e. speed reductions) occurs till the flood depth reaches a certain threshold, and therefore is more realistic.

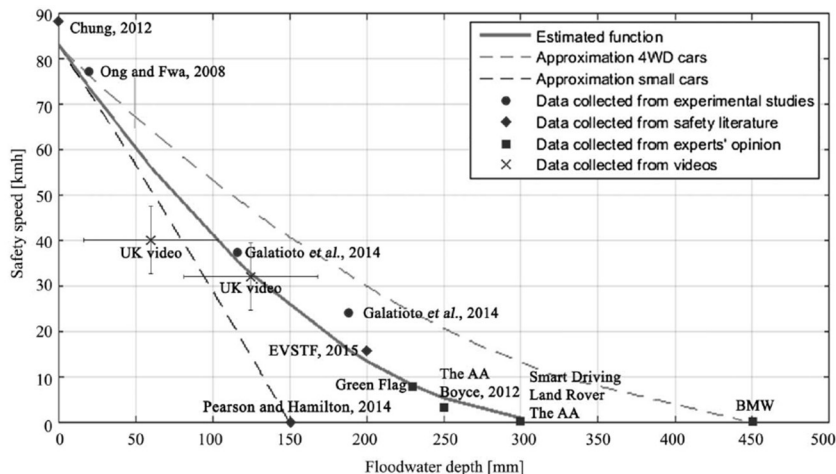


Figure 2.11 Disruption function (Pregolato, 2016).

This depth-disruption function was used by Pregnotato et al. (2017) to assess the impact of climate change on flood-induced disruption to the road network in Newcastle upon Tyne, United Kingdom. They had used a framework combining the hydrodynamic model City Cat with a GIS-based transport model (Fig. 2.12).

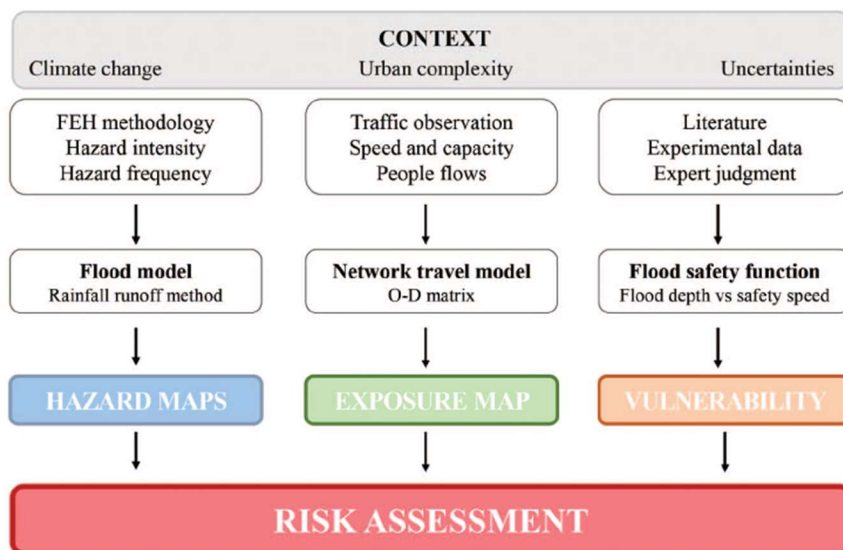


Figure 2.12 The framework to assess pluvial flood-induced disruption to the road network used in Pregnotato et al. (2017).

Their results suggest that travel delays of 13650 and 19446 person-hours in current climate can increase by up to 43% and 66% by 2080 for 10- and 50-year return levels precipitation events (table 2.4).

Table 2.4 Total Person Hour for the 10- and 5-year events (Pregnotato et al., 2017, (modified)).

	Present PHD	2080s PHD
50-year events	13650	19446
10-year events	19446	32363

2.4 Urban traffic demand modelling

Transport demand models are used to simulate traffic characteristics on road networks. These models may be categorized based on a number of characteristics, such as the level of aggregation of the measured data.

The classic four-stage transport model is a well-established framework to simulate travel demand in a transport network on a macro scale. It starts by disaggregating the study area into traffic analysis zones (TAZs) that should be similar to the zones with available demographic information for more accuracy in the data assignment. TAZs are represented by their centroids, which are considered to produce and attract trips as origins and destinations in the road network. The input data required for such models include but is not limited to demographic information, such as the population of different ages and genders; economic information, such as employment conditions, commercial areas, salary range, occupation type, number of cars; social conditions; and other similar information. Such data should be collected for the current and future periods for which the modelling is performed.

The first step in the four-stage classic model is trip generation. This is where information about the TAZs and statistical methods are used to determine how many trips are made and drawn to each TAZ. The second step is to distribute the generated trips between origins and destinations to identify the number of trips between each pair of origins and destinations, the outcome of which is the origin-destination matrix (O-D matrix). In the next step, the produced O-D matrix is assigned to different modes of traffic, such as public transit, active transportation, and private cars. In the last step, traffic assignment is performed to assign the obtained O-D matrices of each traffic mode

to the transport network. Traffic assignment is done to reach an equilibrium traffic state on the road network. The framework is depicted in Fig. 2.13.

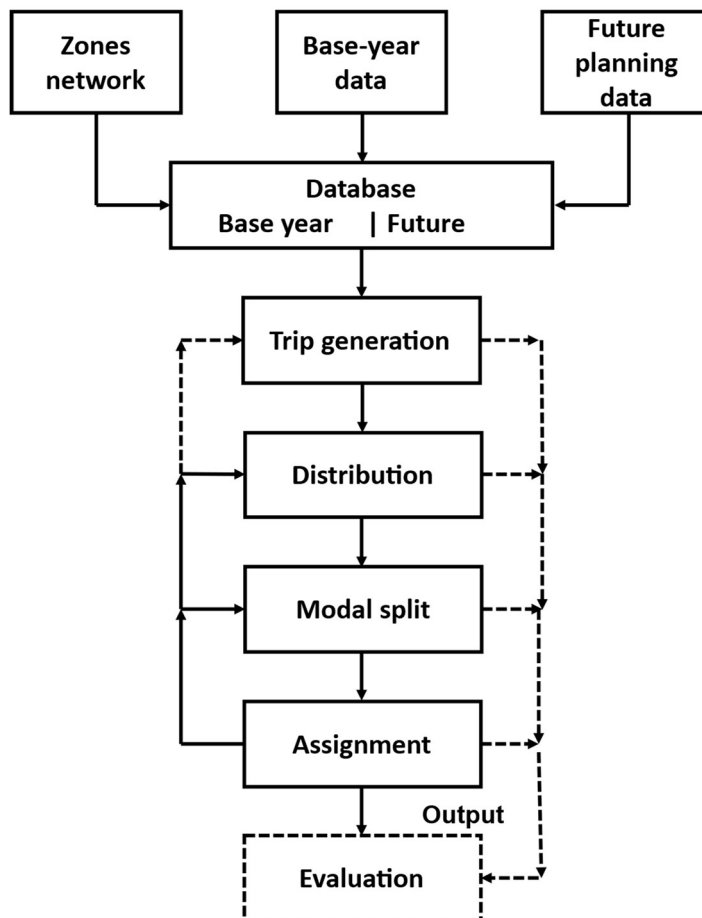


Figure 2.13 The four-stage transport model (Ortúzar and Willumsen, 2011).

The classic four-stage model may not represent the actual situation because the trip makers respond to the transport network conditions. For example, one may refrain from using heavily loaded modes of transport; alter the departure time and path due to the presence of congested links and a lack of parking spaces; and change the frequency of trips or the destination to make the trips less time-consuming (Ortúzar and Willumsen, 2011). Also, the trip makers' responses could be long-term, such as migrating to regions of a city with higher accessibility to commercial,

economic, or recreational areas. It should be noted that the trip generation stage does not take into account the serviceability of the transport system (Ortúzar and Willumsen, 2011).

A critical drawback of the four-stage model is the inconsistency between the attributes fed into the model at different stages of the modelling process. For example, the travel times utilized in the trip distribution and mode split phases may not be the actual values obtained from the last step in the trip assignment phase. The iteration of the processes using the updated values from the previous iterations could be seen as a practical solution, although it comes with computation and run-time costs (Ortúzar and Willumsen, 2011).

The trip generation, trip distribution, mode split, and trip assignment are not the only possible sequences in the four-stage model. This depends on the utility functions that apply to real-world situations (Williams, 1977). It is possible to implement the mode split before performing the trip distribution. The other alternative is to perform the two phases simultaneously. In the first case, the results could be considered an average of the mode split and trip types since the trip generation attributes were more important to the decision-making process (Ortúzar and Willumsen, 2011).

The transport demand models could be categorized as micro or macro models depending on the level of aggregation of the modelling processes and data. The application of aggregate models was popular until 1970, and from the 1980s, disaggregate models became more applied due to the significant advancements they provided. The classic four-stage model is an example of the former, and the activity-based models are considered micro-level simulations. While the activity-based models provide more details about the trip makers and yield more accurate results of the travel patterns, the classic four-stage model is still the most popular transportation demand modelling approach (Zhong et al., 2015). The majority of Metropolitan Planning Organizations (MPOs) use

macro models (Zhong et al., 2015). Even so, some MPOs have started to make micro models to improve the models they are already using (Zhong et al., 2015).

In aggregate models, the primary focus is on the groups of trip makers as opposed to individuals who participate in the unique activities, while in disaggregate models, each individual is simulated based on their unique properties and behaviors. The activity-based travel demand modelling is based on travelers' spatial and temporal behavior (Ilägerstrand, 1970), in which individuals' activities are represented by their participation in economic, social, and other affairs. Aggregate models may be considered rather inaccurate compared to disaggregate models, while the latter may not be capable of estimating detailed information about travel behaviors, especially in the future (Ortúzar and Willumsen, 2011). Also, the statistical and economic skills needed in a disaggregate model are far higher than in aggregate models (Ortúzar and Willumsen, 2011). In certain situations, one needs to plan for future travel demand or to analyze an alteration in a specific variable or the application of a new system. Such practices rely on the travel behavior and properties of the population, not individuals, and require a certain level of aggregation where a macro-level model is applicable.

Research has been undertaken to compare the efficacy of micro-level to macro-level simulations. Chapleau and Morency (2005) have implemented an activity-based travel demand model for Montreal, considering the temporal variation of the population in the central business areas using temporal variations in land use information such as employment. Therefore, the micro-level simulations could yield more accurate results at different times of the day than the aggregate models. Walker (2005) compared the two models in Southern Nevada. He concluded that the application of disaggregate models paved the way to considering detailed demographic

characteristics, such as a population with specific properties, which could be utilized in policy-making practices. (Zhong et al., 2015) compared the applications of activity-based and traditional four-step models in the Tampa Bay Region in Florida. Their analysis showed a big difference between the two models in each of the four stages. They concluded that using an activity-based model, which is more responsive to policies, would help the macro-level simulation be more accurate and work better.

The question of whether to choose an aggregate or disaggregate model can not be answered by a decisive procedure. One needs to clarify the goals of the modelling practice, the level of detail needed, and the level of effort to come up with the correct answer.

2.5 Knowledge gaps and conclusions

Information on projected changes to PFFs and hotspots of traffic disruption is key to the development of adaptation and traffic planning. Realistic modelling of precipitation events, responsible for PFFs, using ultra-high resolution climate simulations are emerging, but such simulations are still lacking over Canada. Extreme events such as PFFs do not occur frequently (even though they have been on the rise recently) and not much observed data on flood depth and their impacts on infrastructures are available in most municipalities. Such deficiencies render it extremely difficult to calibrate hydrodynamic flood models such as PCSWMM with respect to spatiotemporal flood extent, flood depth, and velocity and to calibrate transport network models with respect to actual traffic characteristics in a flooded condition. Qualitative assessments are therefore generally done and efforts should be made in collecting more data related to these events. Furthermore, literature on the impact of PFFs on the transport network and the incurred disruption

is not abundant, especially for Canada. Also, very few studies have integrated ultra-high resolution climate modelling, flood modelling, and transport modelling.

This thesis addresses some of these knowledge gaps by (1) developing a framework integrating ultra-high resolution climate modelling, flood modelling, and transport demand modelling and (2) by assessing the impact of climate change on PFF-induced traffic disruption for the Canadian city of Ottawa.

CHAPTER 3 – FLASH FLOOD-TRAFFIC INTERACTION STUDIES FOR THE CITY OF OTTAWA

Keihan Kouroshejad*, Laxmi Sushama¹

¹ Department of Civil Engineering, Trottier Institute for Sustainability in Engineering and Design, McGill University, Montreal, QC, Canada

*Corresponding author

E-mail: keihan.kouroshejad@mail.mcgill.ca

ABSTRACT

Flash flooding from short-duration high-intensity precipitation events is the predominant cause of weather-related traffic disruptions in summer, which is particularly important for urban areas due to the presence of highly impermeable surfaces such as pavements and buildings. The likelihood of such flash flooding events is expected to increase in a future warmer climate, which can further exacerbate traffic disruptions. This study investigates flash flood-traffic interactions for current and future climates for Ottawa, the capital city of Canada, by integrating ultra high-resolution (4 km) regional climate model (RCM) simulations with inundation modelling using PCSWMM – an urban storm water modelling tool, and exposure analysis based on transport network modelling. Flash floods associated with 100-year return levels of short-duration (i.e., 1-h, 3-h, and 5-h) precipitation events are considered in this study, with the projected changes to the return levels of precipitation estimated using two approaches: in the first approach projected changes are obtained directly from the RCM simulation, while in the second approach, these are obtained using temperature scaling (TS), which is recommended for practical applications.

Quantitative validation of the RCM-simulated precipitation characteristics, i.e. intensity-duration relations for selected return periods and their spatial variability, against gridded and station observations, along with qualitative validation of the hydrodynamic model simulated flash flood depths for past flooding, confirm suitability of the models in analyzing flash flood-related traffic disruptions. Projected increases in the 100-year return levels of 1-h, 3-h, and 5-h precipitation events in the 16-55% range over the study region for the future 2081-2100 period with respect to the 1991-2020 period, for RCP8.5 scenario, suggests increases in the total length of blocked roads, i.e., roads with flood depths higher than 30 cm, in the 24 to 36 km range. This would translate to traffic disruption increases in the 57 to over 77% range, corresponding to delays in the 28,000 to 38,000 person-hour range, which is significant for the City of Ottawa. Thus, by identifying the road links that are susceptible to flash flood related traffic delays through a systematic combined analysis of flash flood-traffic interactions, this study provides a practical framework for generating the required crucial information for guiding the development of adaptation measures to increase resilience in the urban transportation network.

Keywords: Flash floods, Traffic disruption, Climate change, Ultra-high-resolution regional climate modelling, Inundation modelling, Transport network modelling

3.1 Introduction

Urban areas have been identified as vulnerable to various types of floods due to rapid urbanization, population growth, and insufficient drainage systems. Such flood events can lead to loss of lives and detrimental effects on urban systems, such as disruptions to the urban networks and damage to infrastructure. An important factor that contributes to intensifying flood risk in urban areas is the higher fraction of impervious surfaces. Moreover, climate change is projected to increase the intensity and frequency of extreme weather events, such as extreme rainfall (IPCC, 2013), which can further exacerbate urban vulnerability to flood events.

The transport network, which occupies a large fraction of the urban surface area, is an essential component for the efficient operation of urban systems, which can be heavily impacted by Pluvial flash floods (PFFs), as witnessed across many urban centres around the world, including Canada; PFF is associated with short-duration (i.e., sub-hourly to sub-daily) high-intensity precipitation events. The rapid nature of PFFs underpins the fact that there is not sufficient time for measures to be taken shortly prior to an event, making urban areas even more vulnerable to PFFs. Therefore, it is important to understand various characteristics of such events in current climate and how they may change in a future warmer climate in order to identify vulnerable regions, and to devise appropriate adaptation strategies.

In addition to traffic disruptions during PFFs, caused primarily by high flood water depths on the road links, these events can also impact the structural integrity of the transport infrastructure, leading to permanent or temporary failure. PFF-related traffic disruptions can lead to increased travel time and delays, vehicle emissions, and fuel consumption (Mao et al., 2012). Such impacts

are not only restricted to flooded areas, but can also propagate to other regions (Dalziell and Nicholson, 2001; Zio, 2016) and other modes of transport (Fu et al., 2014; Houghton et al., 2009).

While a number of studies have investigated the impact of various weather conditions (e.g., ice, wind, precipitation) on traffic flow and safety (Agarwal et al., 2005; Hooper et al., 2014; Jaroszweski et al., 2010; Kyte et al., 2000; Koetse and Rietveld, 2009; Tsapakis et al., 2013), relatively fewer studies have looked at flood depth impacts. The studies that did analyze the impact of flooding on road closure and safety lack a network-wide analysis of traffic to assess the travel times and delays (Andrey et al., 2003; Chung et al., 2005; Dalziell and Nicholson, 2001; Eisenberg, 2004). For instance, Chen (2008), Su et al. (2016) and Park and Kwak (2011) implemented a microscale approach to assess the impact of PFFs on the road network. City-wide study and planning of transportation networks require macro-scale simulations. Versini et al. (2010) studied the impact of flash floods on the road network for the Gard region in France and used a hydrologic model to implement a road inundation warning system. Yin et al. (2016) combined hydrodynamic model outputs with static transportation network to assess road traffic disruption caused by pluvial flash floods for the city center of Shanghai, China. Their approach lacks sufficient precision and details needed to account for a realistic flood-induced disruption to the traffic network. Li et al. (2018) assessed the impact of PFFs on the road network of Shanghai, but did not consider the spatial variability of rainfall and dynamic modelling of the drainage network. Moreover, in their study, traffic is impacted only for flood depths exceeding a predefined threshold, when complete blockage is assumed. This is not a realistic assumption as any depth of water can impact traffic flows through reduced speeds causing delays in the road network.

Pregnotato (2016) developed a depth-disruption function, based on earlier research that studied the impact of flood flow and velocity on static vehicles (Shu et al., 2011; Xia et al., 2011, 2014),

relating the safety speed of vehicles to water depth on the road links and applied this function in their later study focused on the estimation of PFF-related traffic delays for a city in the UK (Pregolato et al., 2017); An integrated framework coupling PFF and transport network modelling was used in this study. Notwithstanding, their research lacks the spatial variation of precipitation, and dynamic modelling of the drainage network. Spatial variability of precipitation is important and for current climate it can be obtained from observation stations, gridded datasets or reanalysis products. However, sub-daily or sub-hourly information is not always available from observation stations and gridded datasets. These are available for reanalysis products, but at coarse resolutions. A good compromise would be to use credible high resolution climate models.

Regional climate models (RCMs) are generally used to dynamically down-scale global climate model outputs (GCMs) for use in adaptation studies. However, the resolution of RCMs, which is generally in the 10 to 20 km range, is still coarse for engineering applications, as engineering-relevant climate variables such as convective precipitation are not resolved. However, due to the rapid advances on the high performance computing front, convection-permitting models (CPMs) have gained much attention in recent years. Convection-driven short duration high-intensity precipitation events are better represented in these models. Moreover, CPMs have the added benefit of enhancing the depiction of fine-scale orography and surface heterogeneity compared to RCMs (Prein et al., 2013a, 2013b). These ultra-high resolution models can be used to produce climate information at engineering scales that are essential to analyze climate-infrastructure interactions. Kendon et al. (2012) compared ultra-high resolution CPM with coarser-resolution RCM and demonstrated the significant added value of CPM in simulating high intensity rainfalls. Similar results were also shown by Teufel and Sushama (2022) in their CPM study for the

Canadian Arctic region. Therefore, such high-resolution climate modelling is necessary for modelling PFF events.

The main purpose of this study, therefore, is to develop an integrated framework consisting of ultra-high resolution climate modelling, hydrodynamic modelling and transport network modelling to study PFF-related traffic disruptions, in current and future climates, for the city of Ottawa in Canada. The generated information on hot spots of traffic disruptions and delay times will be useful in guiding traffic planning and adaptation strategies.

This paper is organized into 4 main sections, including the introduction. Section 2 gives details of the climate, hydrodynamic, and transport models, observation datasets used for validation, and the methodology used to estimate PFF-induced traffic disruption. Section 3 discusses validation of climate and hydrodynamic models and assessment of projected changes to PFF characteristics and associated traffic disruption. Summary and conclusions of the study are provided in Section 4.

3.2 Models and Methods

3.2.1 Models

The PFF-traffic interaction analysis for current and future climates undertaken in this study is based on the integrated framework consisting of the ultra-high resolution regional climate model GEM (Côté et al., 1998), hydrodynamic model PCSWMM (by Computational Hydraulics International (CHI)) and GIS-based transport network model. The study region comprises the eight inner wards of the City of Ottawa, which includes parts of the Rideau, Mississippi, and South Nation River watersheds (Figs. 3.1b-3.1c).

The GEM model considered in this study is used by Environment and Climate Change Canada for numerical weather prediction. It has also been applied in several previous climate change related studies, including at ultra-high resolution (e.g., Diro and Sushama, 2020; Teufel and Sushama,

2022). The GEM version considered uses the Canadian LAnd Surface Scheme (CLASS; Versegny, 2011) for representing the land surface. This scheme includes prognostic equations for energy and water conservation and allows for a flexible number of soil layers and thicknesses. Other details of the model can be found in Teufel and Sushama (2022). Three GEM simulations at 4 km resolution are considered in this study: The first simulation spanning the 1991-2020 period, over a domain consisting of 340x385 grid cells, is driven by the fifth generation European Centre for Medium-Range Weather Forecasts (ECMWF) reanalysis ERA5 (Hersbach et al., 2020) at the lateral boundaries. This simulation, which is used for validation purposes, will be referred to as GEM_ERA5, hereafter. The other two simulations, spanning the 1991-2020 and 2081-2100 periods, are driven by the Canadian Earth System Model (CanESM2; Arora et al., 2011). Given the coarse resolution of CanESM2, a grid-telescoping approach is used. CanESM2 is first downscaled over the Pan-Canadian domain comprising 580x460 grid cells, at 10 km resolution, the outputs of which are used to drive the same 4 km resolution domain discussed earlier. These two simulations will be referred to as GEM_CanESM2 and will be used to assess future projected changes. The future climate simulation here corresponds to IPCC's Representative Concentration Pathway (RCP) 8.5 scenario.

The flow depths and velocities of PFFs required to estimate traffic disruptions are estimated through PCSWMM. This model, which is based on the EPA SWMM, developed by Canada Computational Hydraulics International (CHI), is capable of integrated 1D-2D hydrologic-hydraulic modelling. It is widely used in urban drainage and rainfall-runoff studies, and in the assessment of Low Impact Developments (Peng et al., 2019). For the purpose of this study, the overland grid of PCSWMM is configured at 25-meter resolution considering the computational resources available, with sub-catchment parameters defined based on land-use, soil, and

topographic data and relevant recommended values from literature. The drainage network for the study region is dynamically replicated in the model by specifying pipeline shape and cross-section, offset value, start and end locations, invert elevation of manholes, maximum depth of manhole, and other network characteristics, which were obtained from the City of Ottawa.

The road traffic disruptions associated with PFFs are estimated over the study region using a GIS-based transport network model, which computes the shortest paths between each pair of origin and destination (represented by the centroids of the wards, producing and attracting trips) based on travel times. The number of trips between the eight pairs of origin and destination, are derived from the auto driver mode origin-destination data from the latest origin-destination survey for the evening peak hour, for all trip purposes. In the model, roads and junctions are represented with a set of links and nodes, obtained from Canada National road network database. Road classes, capacities, free-flow speed, and BPR (Bureau of the Public Road) speed-flow curves are defined based on the TRANS report (2013). The calibrated BPR functions are implemented inside the model to account for the congestion impact on the traffic flow. Some of the processes inside the model are simplified to ensure that the model is computationally efficient. Local roads are removed from the model given the road users' lack of knowledge of the alternative minor roads and the lower capacities of the local roads, which are conducive to congestion under small loads of traffic. Furthermore, no stochastic variation in traffic is considered in the road network. Traffic assignment is performed using an iterative procedure based on the computed shortest paths to reach equilibrium traffic flow conditions on the road network.

For no flood case, speeds are derived from the speed-flow curves to account for the impact of congestion on traffic flows. For flood cases, modelled flood depths in conjunction with a disruption function (Pregolato et al. 2016) associating floodwater depth and the reduction in the safety speed

is used to assess the integrated impact of traffic congestion and floodwater depth on traffic speed; the minimum speed from the speed-flow curve and the disruption function is used. The disruption function shows that safety speed decreases as the floodwater depth increases, which is more realistic than the only assumption that road links are entirely blocked or operational under flooded conditions, which has been adopted in some studies.

3.2.2 Methods

The current and future PFFs considered in this study correspond to 100-year return levels of 1-h, 3-h, and 5-h precipitation events; The Chicago method (Keifer and Chu, 1957) is used for obtaining design hyetographs as required by PCSWMM. The 100-year return level is selected as the main focus of this study is on traffic disruptions associated with PFFs. Such a high return level is generally not considered in the design of drainage networks, which are designed for much smaller return levels (e.g., 2- to 5-year return levels). Two methods are used to derive current and future return levels. In the first approach, they are derived directly from GEM_CanESM2 simulations. In the second approach, the return levels for current climate for the three precipitation durations considered in this study are estimated for the OTTAWA CDA RCS observation station (45°23'N and 75°43'W), which is the only station with hourly data within the study region. Temperature scaling (TS) (Eq. 1) is applied to the observed return levels to estimate future return levels, following the recommendations from Environment and Climate Change Canada, the Canadian Highway Bridge Design Code, and the National Building Code of Canada (CSA PLUS 4013) as:

$$R_F = R_C \times 1.07^{\Delta T}, \quad (1)$$

where R_F is the future return level, R_C is the current return level, and ΔT is the projected temperature change between the current and future periods, which in this study is derived from the

GEM_CanESM2 simulations. Note that, in the first approach, return levels vary in space, while it is constant in space in the second approach. The first approach is conservative in that the probability of simultaneous occurrence of design storms at various grid cells is low as they are produced from different events.

The traffic disruption in this study is estimated in terms of Person Hour Delay (PHD) as:

$$PHD = PH^F - PH^{NF}, \quad (2)$$

where PH is the travel time for all trips for all origin-destination pairs considered and is given by

$$PH = \sum_{i=1}^N \sum_{j=1}^N T_{ij} C_{ij}. \quad (3)$$

Here, T_{ij} is the number of trips between origin i and destination j , C_{ij} is the cost of trip (i.e., travel time) between i and j , and N is the number of origins or destinations; PH^F and PH^{NF} in Eq. (2) correspond to PH for the flood and no flood cases.

Prior to applying the models (GEM and PCSWMM) for investigating future scenarios, they are validated by comparing against available observations. Where observations are not available, qualitative validation is considered. GEM's ability in simulating precipitation characteristics, both mean and extremes, are assessed by comparing GEM_ERA5 simulated characteristics with those from Daymet (Thornton et al., 2016) gridded dataset and station observations, respectively. Six observation stations within and near the study region are selected for validation, which will give a more general idea about model performance. PCSWMM is validated qualitatively by comparing regions of high flood depths with accumulation-prone areas according to DEM for a historic event of July 1, 2017. Projected changes to traffic disruption are assessed by comparing the PHD in future climate with that for current climate, for the precipitation durations considered in this study and for the two approaches used for deriving return levels.

3.3 Results

3.3.1 Validation

The spatial patterns of summer mean precipitation simulated by GEM-ERA5 compared with Daymet in Fig. 3.2-a show some overestimation (1mm/hr) in the centre of the domain. The underestimation along the southern and western boundaries are primarily due to a boundary effect of the driving data and is in the 2 mm/hr to 3 mm/hr range. The study region, which is far from the boundaries has errors less than 1 mm/hr. This comparison between GEM_ERA5 and Daymet is indicative of performance errors, i.e. errors associated with the model. The results for GEM_CanESM2, for current climate, is very similar to that for GEM_ERA5, except for a slight increase in the overestimation. The comparison of GEM_CanESM2 and GEM_ERA5 points to the errors associated with the driving CanESM2. Overall, the impact of the boundary forcing data does not seem to be large.

Since the main precipitation characteristics of interest are the 100-year return levels of short duration precipitation events, the intensity-duration relations obtained from GEM_ERA5 and GEM_CanESM2 are compared to those with six station observations (Fig. 3.2-b). The GEM simulated relations are very similar to those observed, although overestimation of the relation is noticeable for GEM_ERA5 for two stations (ANGER and Montreal PIERRE ELLIOTT TRUDEAU INTL) and for one station (OTTAWA CDA RCS) for GEM_CanESM2. Overall, the comparisons provide confidence in applying GEM in future climate simulations. Furthermore, the model has previously been validated in a number of studies, which confirmed the model's ability in representing precipitation characteristics, and also demonstrated improved simulation of short-duration high intensity precipitation events in summer at ultra-high resolution (Teufel and Sushama, 2022).

Validation of PCSWMM is accomplished qualitatively by studying the flood characteristics for the flash flood event of July 1, 2017. The precipitation event as captured at the observation station is shown in Fig. 3.3-a. The event as simulated by GEM_ERA5 at the representative grid cell containing the observation station, shown in the same figure, suggests that, although the peak is slightly shifted in GEM_ERA5, the event – peak magnitude, event duration and volume – is overall well captured. PCSWMM, driven by GEM_ERA5 simulated precipitation event (which vary in space), simulated floodwater depth (Fig. 3.3-b) shows higher values, particularly in the southern regions where the precipitation magnitude is higher (figure not shown) for this specific event. Moreover, PCSWMM simulated flood water depth is higher in low-lying areas, identified using the DEM (Fig. 3.3-c), compared to the surrounding regions, which is in accordance with what is expected. Lack of any additional observed data (flood depth and velocity) related to this flood event limits comparison, but the qualitative comparison provides some confidence in the model and model parameters for application in this study.

3.3.2 Projected changes to PFF characteristics

As discussed under Section 2, two approaches are used for estimating projected changes to the precipitation return levels considered in this study. Results based on the temperature scaling approach will be discussed first followed by that based directly on GEM_CanESM2.

In the temperature scaling approach (Eq. 1), the future 100-year return levels corresponding to 1-h, 3-h and 5-h precipitation events at the Ottawa CDA RCS observation station is estimated using current observed return levels and temperature change obtained from GEM_CanESM2 simulations for the most representative grid cell. This temperature change for the period 2081-2100 with respect to the 1991-2010 period is 6.48°C for the considered RCP8.5 scenario. The percentage increase in the return levels using this approach yields same values for all precipitation durations.

Figure 3.4 shows the Chicago design storms corresponding to the 100-year return levels of 1-h, 3-h, and 5-h precipitation events for current and future climates at the observation station. A considerable increase in the overall amount of precipitation and an increase in the peak magnitude, of 108 mm/h for 1-h, 3-h, and 5-h, can be noticed in this figure, from current to future climate.

The corresponding hydrodynamic modelling results from PCSWMM are shown in Figs. 3.5-3.8. Lower values of total runoff simulated by PCSWMM (middle left column of Figs. 3.5- 3.7) in the fringe areas of the study region is due to the relatively higher perviousness and therefore, infiltration in these regions. Projected runoff increases of higher than 20 mm is noted for 1-h precipitation (Fig. 3.5), with higher increases for longer durations of precipitation (3- and 5-h) (Figs. 3.6, 3.7).

The analysis of the drainage network shown in Figs. 3.5-3.8 suggests that under current 100-year flash floods, the max flow to capacity ratios exceeds 1 for several segments, which could be interpreted as surcharged pipes. This is reasonable as the drainage pipes are normally designed for 2 to 5-year return periods of short-duration precipitation events. The total length of surcharged pipes is estimated to be augmented in future climate; for 100-year return level of 1 h events, 49% increase is projected. The same patterns are observed for 3-h and 5-h precipitation events, with a modest increase in the pipeline flows.

The maximum depth of flood (Figs. 3.5-3.7) suggests that 3.14, 5.81 and 9.54 km of the road network can experience depths higher than 30 cm, for 100-year return levels of 1-h, 3-h, and 5-h precipitation events, respectively, in current climate. The speed reductions that can be caused by depths smaller than 30 cm in other segments of the network, combined with the complete blockage for segments where water depth is higher than 30 cm, can cause significant disruption to traffic in

current climate. These are quantified in Section 4. In future climate, 31.15, 41.62, and 44.47 km of completely blocked roads are simulated for 100-year return levels of 1-h, 3-h, and 5-h events. Furthermore, the rest of the road network will experience higher depths in future climate compared to current climate, that can lead to substantial reductions in the travel speed between O-D pairs, causing significant travel delays, which are quantified in Section 4.

The max flood depth assessments based on return levels obtained directly from GEM_CanESM2 are compared with the TS approach here. Comparing flood results for 1-h, 3-h, and 5-h rainfall using GEM-based and TS-based approaches (Fig. 3.8) reveals that the majority of the study area receives almost the same amount of max floodwater depth using both approaches in current climate. Notwithstanding, in current climate, TS-driven simulation shows higher max flood depth in the urban core, whereas GEM indicates higher levels in the outskirts (in the 1 cm to more than 10 cm range). However, future results show the opposite patterns (Fig. 3.8), where the maximum flood depth for TS-driven simulation is lower than that in the GEM-driven simulation for the road links located in the central areas, while higher values are seen in the periphery for the TS case in the range of 1 to 5 cm (Fig. 3.8). These contrasting patterns in future compared to current climate occurs as GEM-based projected changes to precipitation in the urban core (periphery) are higher (lower) than that based on the TS approach which assumes spatially constant rainfall.

Figure 3.9 shows the percentage of road network affected by flash floods for the different cases considered in this study, i.e. 100-year return levels of 1-h, 3-h, and 5-h durations in current and future climates, for both approaches. It is evident that for both current and future climates, as well as for both approaches, the overall percentage of the road network affected by less than 5 cm of water depth decreases with increasing duration. The opposite is apparent for flood water depths greater than 5 cm, where flood water depth increases with increasing precipitation duration. By

comparing results for current and future climates, a projected increase (decrease) in the percentage of the road network with flood depths above (below) 5 cm for both methods is noted. Particularly important is the length of the road network that is projected to be blocked entirely due to water depths higher than 30 cm. Based on the results, this percentage is projected to reach 4 to 6 percent of the total road network in the future compared to less than 3 percent in current climate. Moreover, future results suggest that the total share of the road network affected by less than 1 cm and more than 30 cm of water depth is higher for the GEM-based case. Overall, TS-based and GEM-based results are very similar.

3.3.3 Traffic disruption

Figure 3.10 shows the traffic speed reduction on the road network in percentage for current and future climates for 100-year return levels of 1-, 3-, and 5-h precipitation events using TS-based and GEM-based approaches. In current climate, both methods show that the traffic speed reduction is less than 25% for most of the road network; the number of road links with above 25% reduction is relatively higher for the GEM-based approach compared to that based on TS (Fig. 3.10, first and third row). Generally, traffic speed reduction increases with increasing precipitation duration, with the largest reductions noted for the 5-h event (Fig. 3.10). In future climate, speed reduction is projected for more road links, and the number of links with speed reduction higher than 50% seems widespread for both approaches (Fig. 3.10, second and fourth rows). This implies longer travel times/delays as discussed below.

Table 3.1 displays the person-hour delay (PHD) for the 12 scenarios analyzed in this study. For both approaches, PHD, in general, is higher for higher precipitation durations, in both current and future climates. The PHD values for the GEM-based approach are slightly higher than those for the TS approach in current and future climates. This is consistent with Fig. 3.9, where GEM-based

approach displays higher percentage of the road network affected by depths larger than 30 cm in current and future climates compared to the TS-based results. Although there is not a discernible pattern of difference between the two approaches for other flood depth ranges and even though certain links exhibit the reverse relationship between GEM and TS, the overall effect is controlled by the larger disparities, which reduce the safe speed by significantly larger values and results in the closure of such road segments. Projected increases in PHD, i.e. traffic disruption are estimated to be 58, 59, 57% and 77, 60, 60% for 1-h, 3-h, 5-h precipitation events for TS- and GEM-based approaches, respectively. This shows similar increases in travel delays for both approaches for the 3-h and 5-h events. It should be noted that the overall disruption is not distributed uniformly across the road network and varies based on the volume of traffic and the magnitude of the flood water depth (e.g. see Fig.10). The differences for 1-h duration between the TS-based and GEM-based approaches raises the question of validity of the temperature scaling relation for very short durations, which can benefit from additional studies focused on this topic.

3.4 Summary and conclusion

Projected increases/decreases in flash flood-related road network/traffic disruption for the City of Ottawa for the future 2081-2100 period with respect to the current 1991-2010 period are considered in this study, with the future climate corresponding to the RCP8.5 scenario. An integrated framework consisting of ultra-high resolution (4 km) GEM regional climate model simulations, hydrodynamic model PCSWMM, and GIS-based transport network model are used to this end. The flash flood scenarios considered are those associated with 100-year return levels of 1-h, 3-h, and 5-h precipitation events, which are estimated using a temperature scaling approach as well as using GEM precipitation outputs directly. Satisfactory validation of GEM model's ability in simulating precipitation characteristics, particularly short-duration high intensity precipitation

events, and that of PCSWMM in simulating flood depths confirmed the applicability of these models in achieving the objectives of this study.

Results suggest projected increases in travel delays in the 57 to 77% range from 1991-2010 to 2081-2100 for flash floods associated with 100-year return levels of 1-h, 3-h, and 5-h precipitation events, depending on the approach implemented. This is caused by the overall reduction in speed with higher flood depths for many road links and 3% to 5% increase in road segments where complete blockage due to depths higher than 30 cm are projected for future climate. Most of the hotspots are in low-lying areas and regions with insufficient drainage and/or infiltration.

This study, despite some limitations, provides useful information which can form the basis for additional future studies. For instance, the macro-scale simulation of traffic considered in this study was simplified and does not consider the stochastic variation of traffic on the road links and is based on the premise that all trip makers are fully aware of the network conditions and select the optimized routes. Moreover, vehicle-to-vehicle, vehicle-to-pedestrian, and intersection interactions are not considered. These details could be considered in an agent-based model where behavior of individual vehicles and interactions can be considered.

In conjunction with the dynamic connectivity between the transport model and the hydrodynamic model, an agent-based model could provide greater insight into the consequences of flash floods during the course of a flood. Such information might include the duration of link closures and the time required to return to normal conditions, driver behavior and traffic patterns under flash flood conditions, and the pattern by which a blockage or severe disruption on one road link could propagate to other road links. However, such effects are unlikely to be decisive in a city-level

analysis, and micro-level simulations require substantially more processing resources. Consequently, the estimated travel times are expected to be on the low side.

A number of challenges remain to be solved. Calibration of the hydrodynamic and transport models can be improved by considering many events. However, this entails data from historical events and more computing resources. Furthermore, the ultra-high resolution simulation considered in this study can be replaced with even higher resolution simulations. At 4 km resolution, 24 grid cells cover the study region; spatial variability in precipitation can be better captured at sub-km scales. However, this is computationally expensive and hybrid approaches such as combining GEM model outputs with machine learning approaches can be explored. Furthermore, other emission scenarios and driving GCMs can be considered to better quantify uncertainties. Nonetheless, this study provides useful information regarding flash flood related traffic disruptions for the City of Ottawa in future climate, which can guide and/or stimulate additional studies to inform the development of adaptation and transport planning strategies.

Acknowledgments

This research was funded by the Natural Sciences and Engineering Research Council of Canada (NSERC), Trottier Institute for Sustainability in Engineering and Design (TISED) and McGill Sustainability Systems Initiative (MSSI). The simulations considered in this study were performed on the supercomputer managed by Calcul Québec and Compute Canada. The authors also would like to thank Computational Hydraulics International (CHI) for providing PCSWMM software under CHI University Grant Program and the City of Ottawa for the drainage network data.

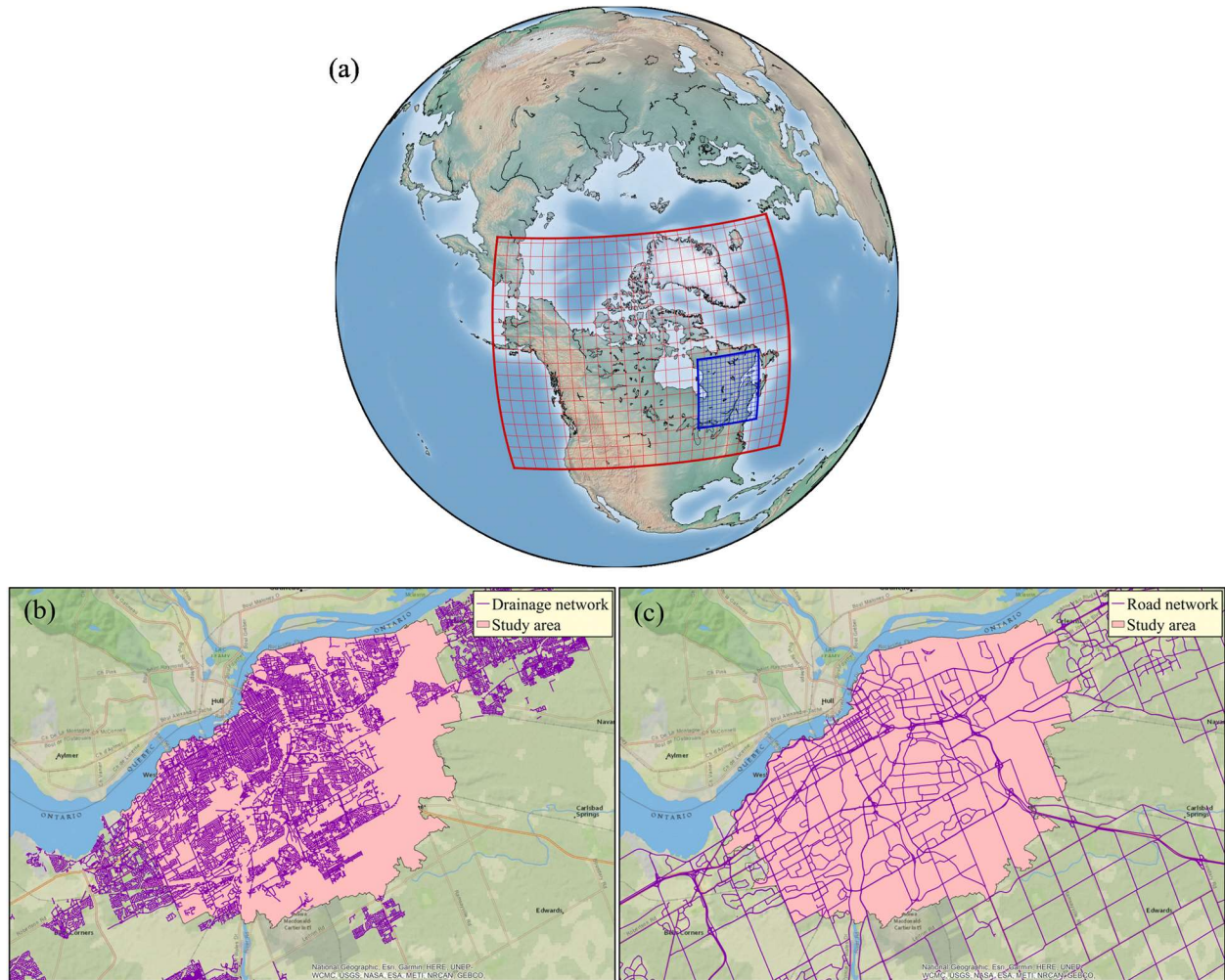


Figure 3.1 (a) GEM experimental domain at 10 km (red) and 4 km (blue) resolutions, with every 25th and 20th gridlines, respectively, shown. (b) The road network and (c) drainage networks for the study domain consisting of eight inner wards of the City of Ottawa (shown in pink).

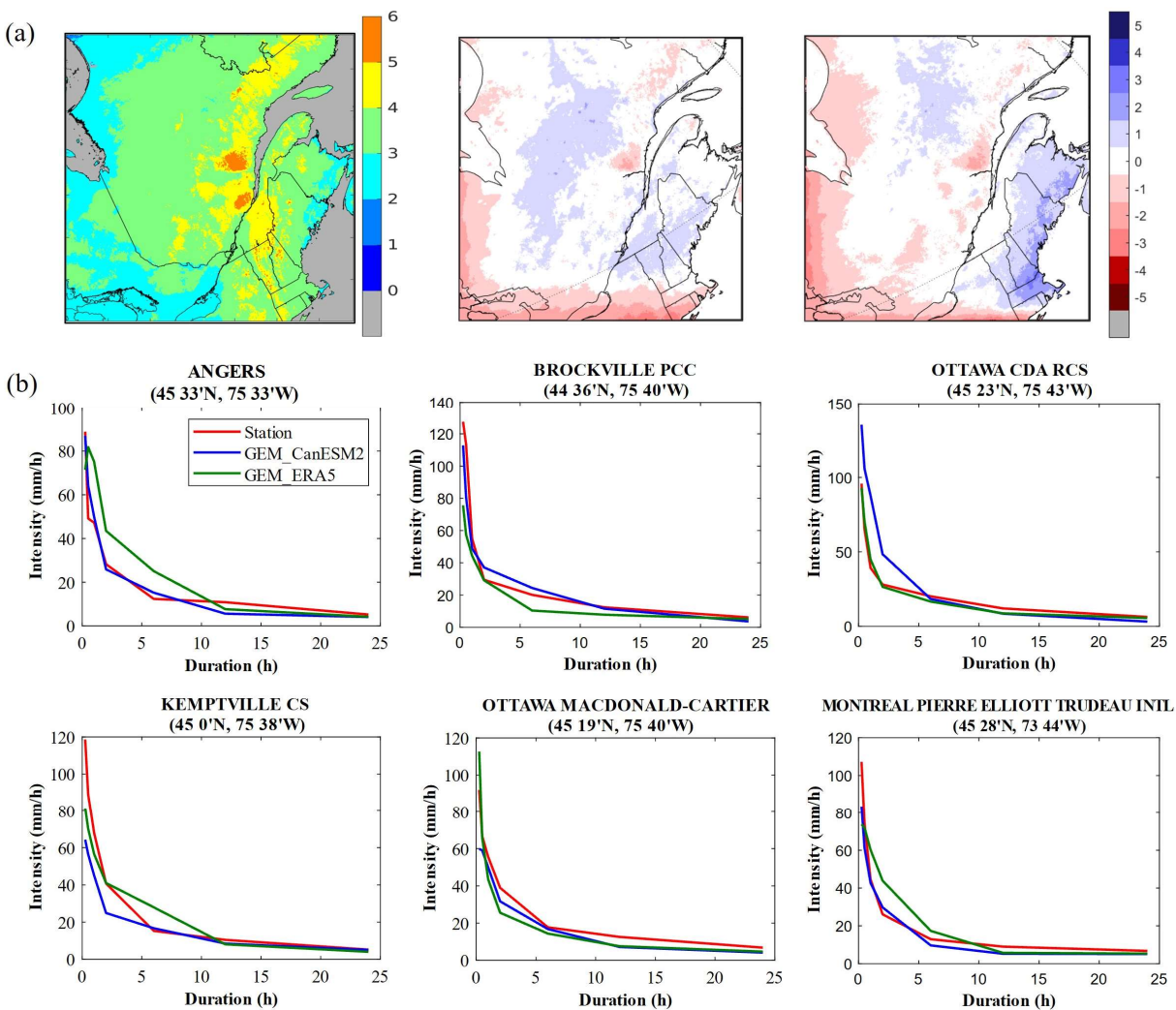


Figure 3.2 (a) Mean summer (June–August) precipitation from Daymet (left panel) for the 1991–2010 period, and GEM_ERA5 (center panel) and GEM_CanESM2 (right panel) biases. (b) Observed, GEM_ERA5, and GEM_CanESM2 simulated intensity-duration relations for 6 stations around the study area.

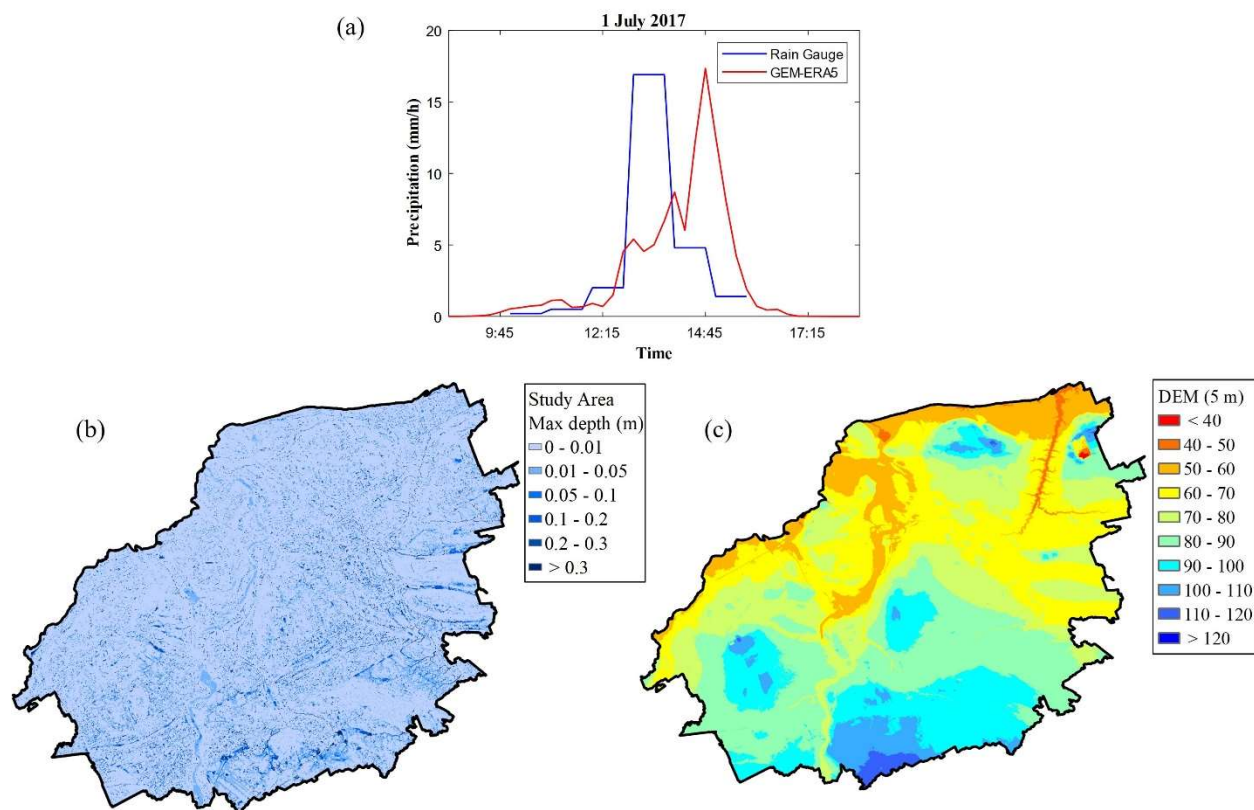


Figure 3.3 (a) The July 1, 2017 observed and GEM_ERA5 simulated precipitation event at OTTAWA CDA RCS. (b) PCSWMM simulated maximum flood depth for the event and (c) Digital Elevation Model at 5 m resolution.

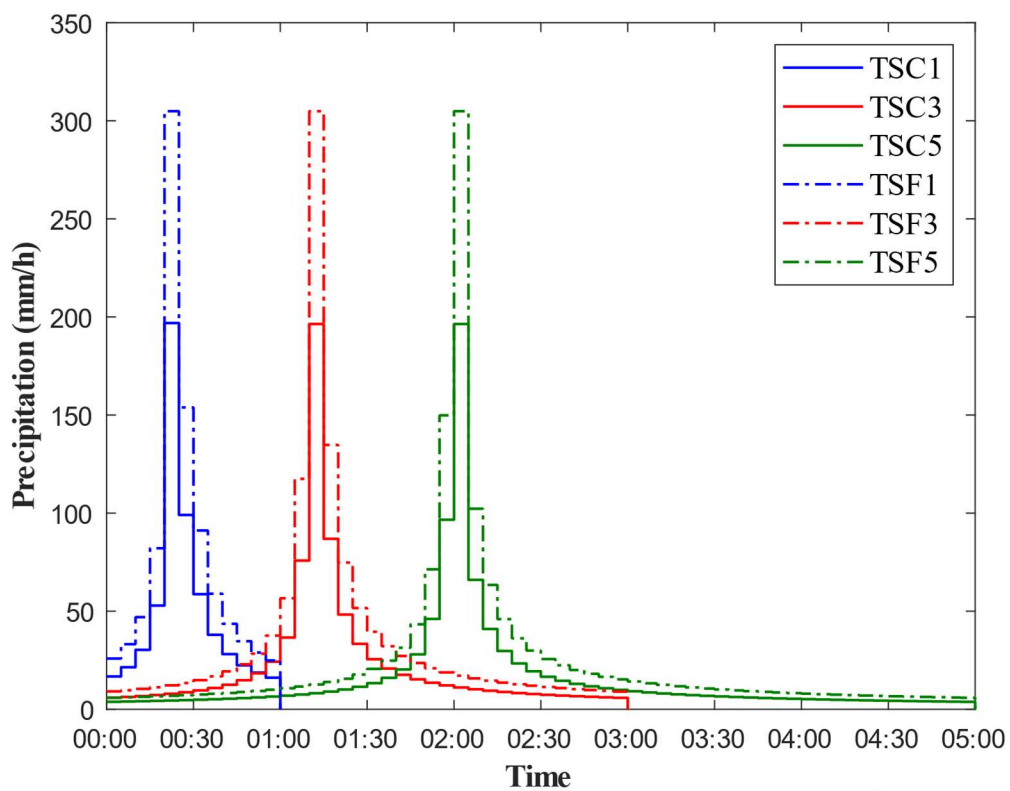


Figure 3.4 Design storms corresponding to 100-year return levels of 1-h, 3-h, and 5-h precipitation events for current (TSC1, TSC2, TSC3) and future climates (TSF1, TSF2, TSF3) at OTTAWA CDA RCS station; Future return levels are estimated using the temperature scaling approach.

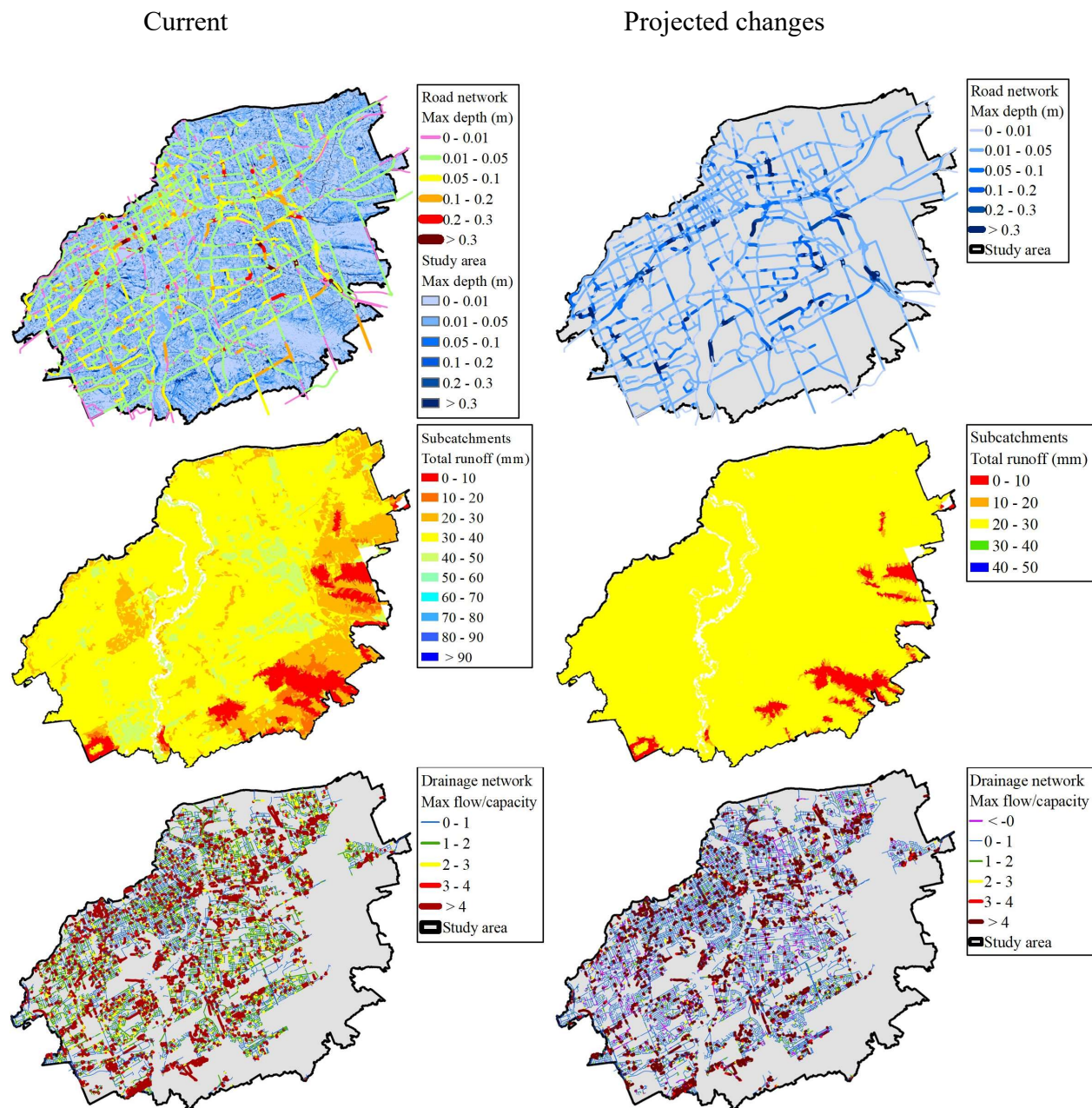


Figure 3.5 Max depth (top), total runoff depth (middle) and sewer max flow/capacity (bottom) for current climate (left column), and their projected changes (right column) for the 100-year return levels of 1-h precipitation for the temperature scaling approach.

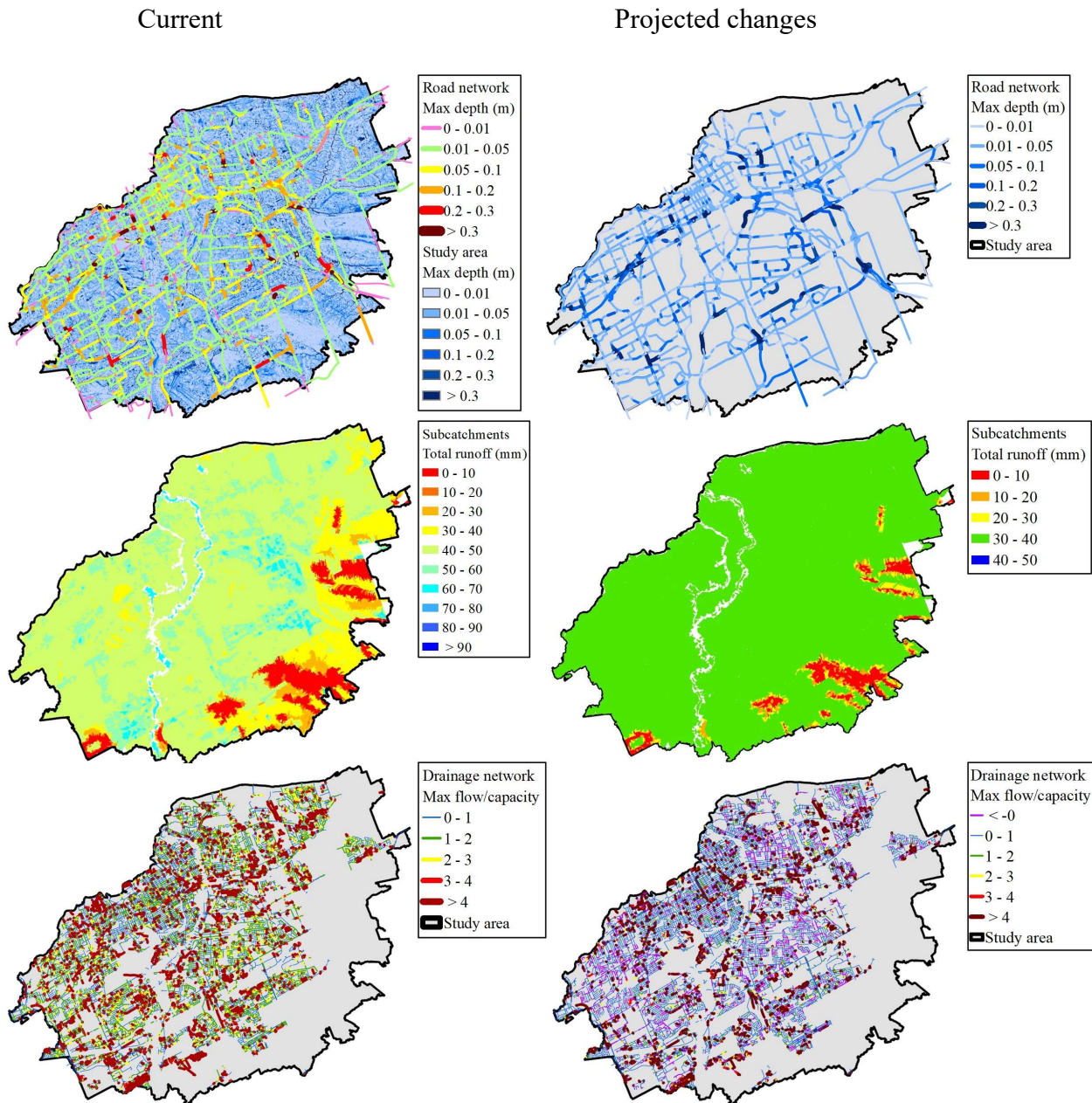


Figure 3.6 Max depth (top), total runoff depth (middle) and sewer max flow/capacity (bottom) for current climate (left column), and their projected changes (right column) for the 100-year return levels of 3-h precipitation for the temperature scaling approach.

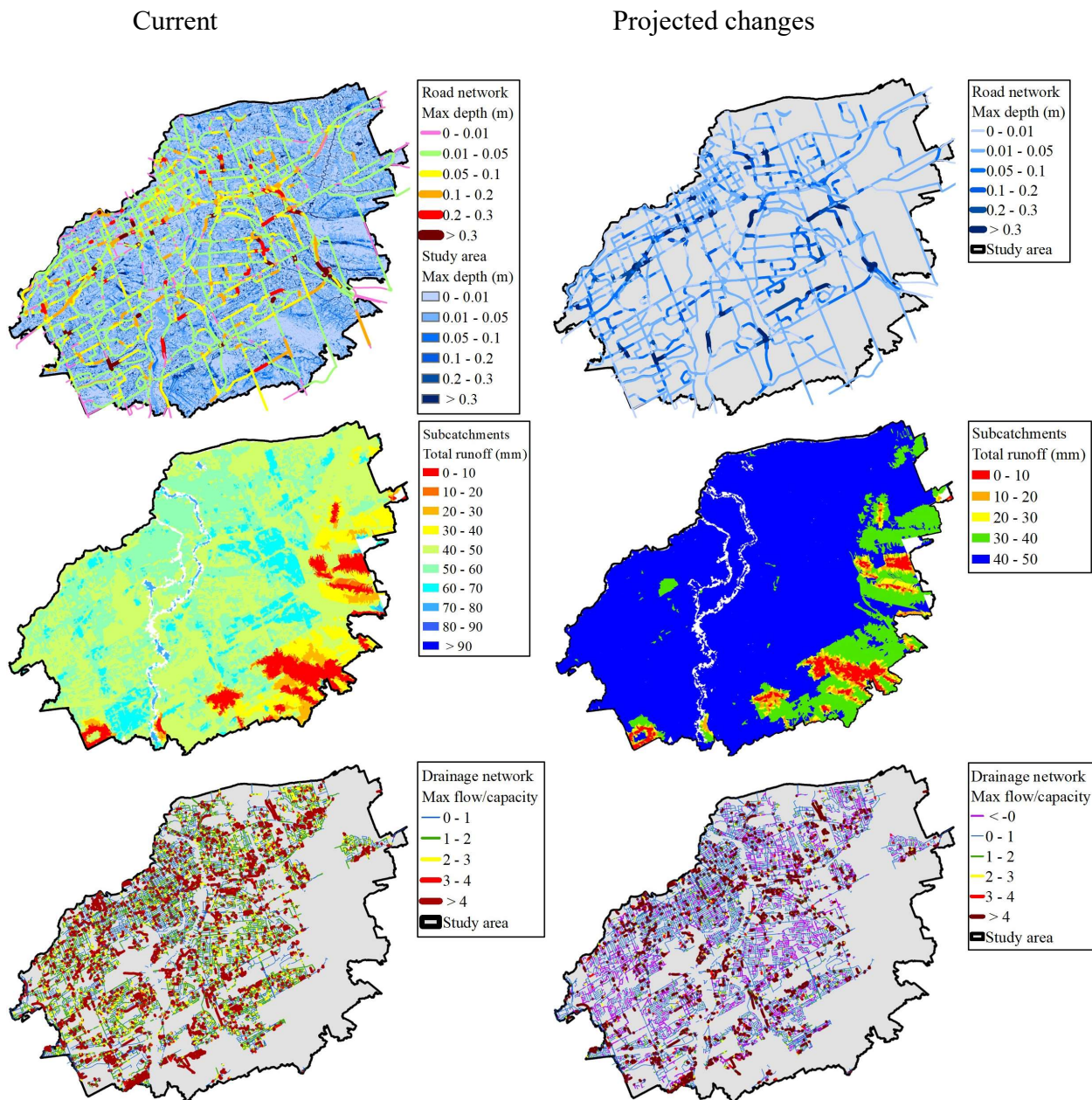


Figure 3.7 Max depth (top), total runoff depth (middle) and sewer max flow/capacity (bottom) for current climate (left column), and their projected changes (right column) for the 100-year return levels of 5-h precipitation for the temperature scaling approach.

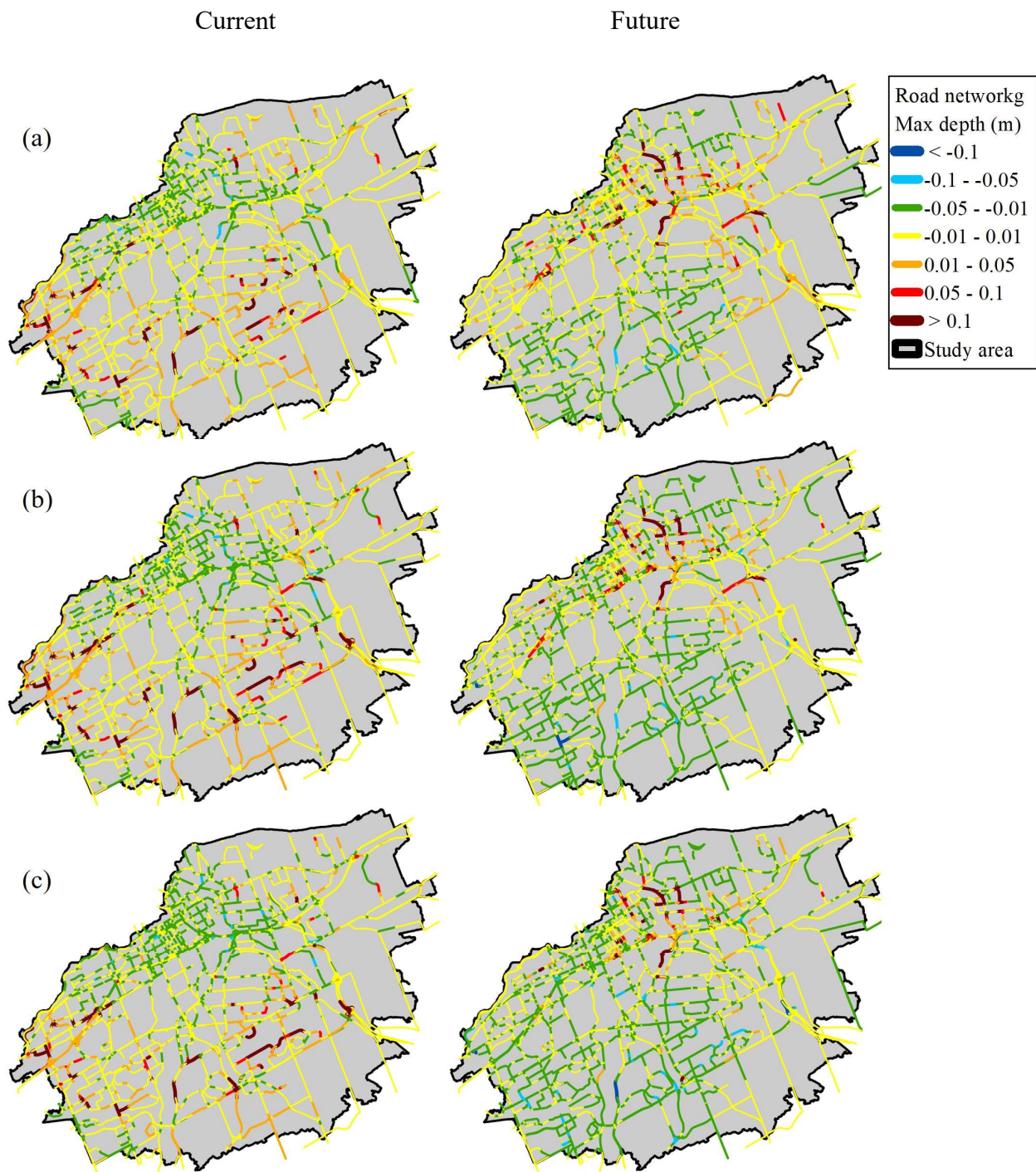


Figure 3.8 Differences in maximum flood depths for the two approaches (GEM-based and temperature scaling-based) for current (left) and future (right) climates for 100-year return levels of (a) 1-h (top), (b) 3-h (center), and (c) 5-h (bottom) precipitation.

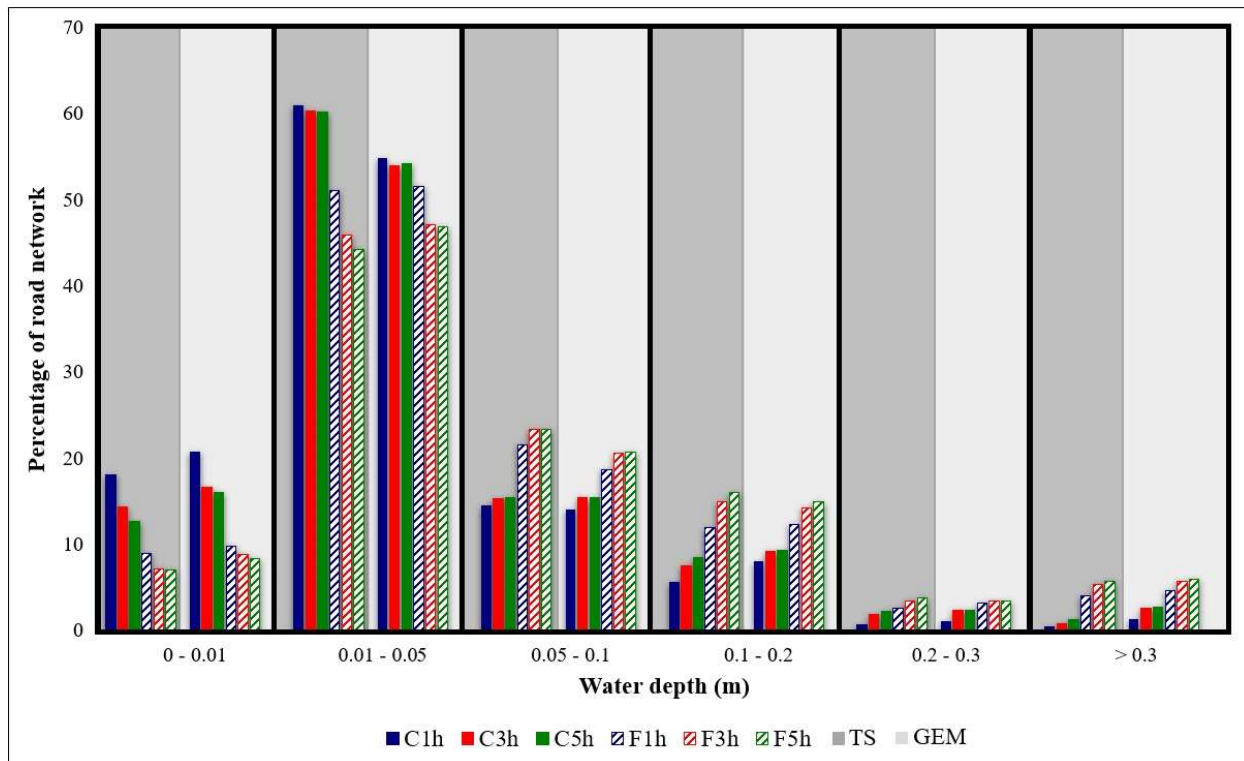


Figure 3.9 Percentage of the road network corresponding to various flood depth bins, for current (shaded bars) and future (hatched bars) climates, for 1-h (blue; C1h, F1h), 3-h (red; C3h, F3h) and 5-h (green; C5h, F5h) precipitation events for the TS (dark grey background) and GEM (light grey background) based approaches.

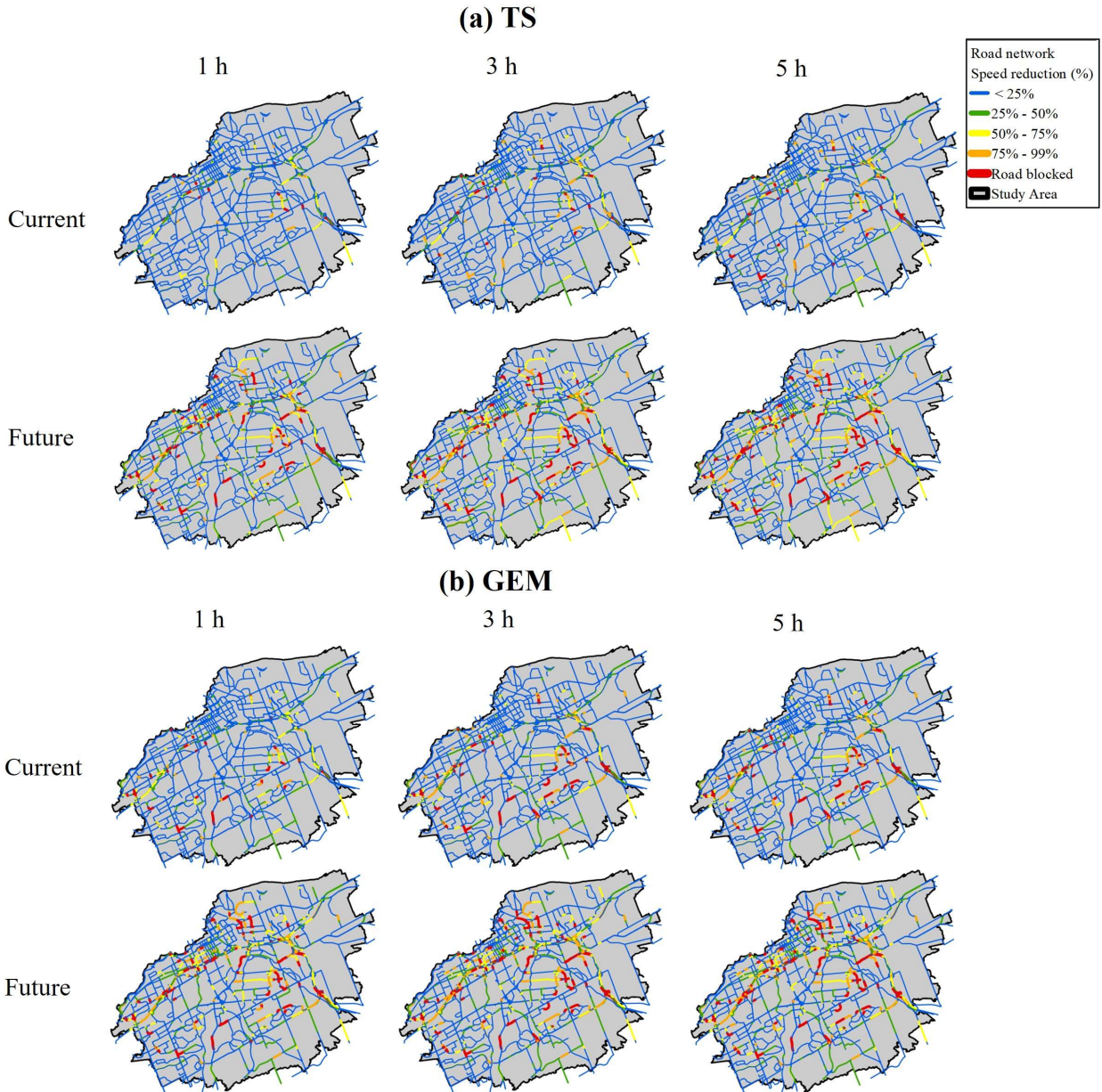


Figure 3.10 Speed reduction (in percentage) for 100-year 1-h (first column), 3-h (second column), and 5-h (third column) precipitation events for current (top) and future (bottom) climates for the (a) TS-based and (b) GEM-based approaches.

Table 3.1 PHD for current and future climates; TS1 (G1), TS3 (G3), TS5 (G5) correspond to temperature scaling-based (GEM-based) approach for 1-h, 3-h and 5-h durations.

	Current	Future	Projected changes
TS1	47951.11	75913.98	58.32
TS3	48335.15	76920.03	59.14
TS5	48895.92	76896.97	57.27
G1	49595.17	87726.27	76.88
G3	55462.52	88678.26	59.89
G5	55204.56	88190.15	59.75

CHAPTER 4 - DISCUSSION

This chapter provides additional discussion on the study's main assumptions and limitations and also explores the added value that can be obtained by employing sub-km resolution climate simulations.

4.1 Assumptions, models, and methods

The framework comprising the ultra-high resolution climate, hydrodynamic, and transport demand models developed as part of this study can be applied in any city provided that essential data is available. This study selected the city of Ottawa as the required data were available, which includes ultra-high resolution (4 km) climate change simulations and data required by PCWSMM, such as the drainage network.

PCSSWMM is selected for hydrodynamic simulation as it is widely applied in hydrodynamic practices and is a powerful tool combining hydrologic and hydraulic modelling. Although computationally costly, the integrated 1D-2D flood modelling is employed to simulate PFF over the study area as it is the most comprehensive modelling method and simulates the overland flows in 2D and the drainage networks and other linear systems in 1D. The overland hydraulic simulation is performed at 25-m resolution. Adopting higher resolutions entails substantially higher computational resources and running time. On the other hand, lower resolutions may lead to inaccurate results, as higher resolutions are required to capture the hydraulic characteristics of local streets. The hydrologic modelling is configured at 100 m resolution, and sub-catchments are delineated accordingly. Adopting hydrologic modelling resolution requires caution as it can impact process representation. For instance, infiltration is a time-dependent process and could be

underestimated if sufficient residence time is not allowed for the runoff in the sub-catchments. This can happen in small sub-catchments where the concentration time is not sufficient. The opposite is valid for large sub-catchments where ample drainage time is present.

Some of the assumptions made in this study can be modified/revisited. For example, this study considered only the traffic disruption to PM peak hour caused by maximum flood depth. It should be noted that this is a rather conservative approach because it is assumed that the PM peak of traffic and max flood depth over the study site coincide. In order to simulate the temporal patterns of traffic disruption, one needs to dynamically link the transport network and the PFF models and consider the variations of traffic and flood depth over time.

This study considers the TS-based and GEM-based approaches for estimating projected changes to return levels. TS-based, although simplified, showed minor differences with those of GEM-based results. For example, the projected changes to 100-year 1-h, 3-h, and 5-h precipitation for 2081-2100 with respect to 1991-2010 for the RCP 8.5 (Fig. 4.1) show that TS projections are higher compared to that based on GEM. TS predicts a 55% increase in return levels irrespective of the duration of the events, while GEM projections for 100-year 1-h, 3-h, and 5-h precipitation suggest increases to be 15.7, 26.38, and 29.7%. However, leaping to conclusions about the resulting disparities between the two modelling approaches based solely on the projected changes to precipitation return levels is naive because several other factors play a role. For example, GEM precipitation is spatially varying, and the above values correspond to the average over the whole study site. In some grid cells, projected increases in precipitation are higher and vice versa. Moreover, GEM results show higher return levels compared to those in TS for some rainfall durations in current climate. For example, 100-year return levels of precipitation for 1-h

precipitation is 65.43 and 49 mm/h for GEM and TS, respectively. Hence, the percentage increase in the precipitation return levels does not necessarily imply more intense traffic disruption in TS than GEM-based method, which was observable in chapter 3. The difference between the two approaches is reflected in the estimation of the simulated projected changes to flood water depth and the resulting travel delays which is discussed in Chapter 3.

Overall, TS is a simplified empirical approach, not differentiating between precipitation durations and return periods, so it can yield unrealistic results compared to physically based models such as GEM, although having its own biases. More studies are needed to verify the validity of TS in simulating projected changes to precipitation over different regions.

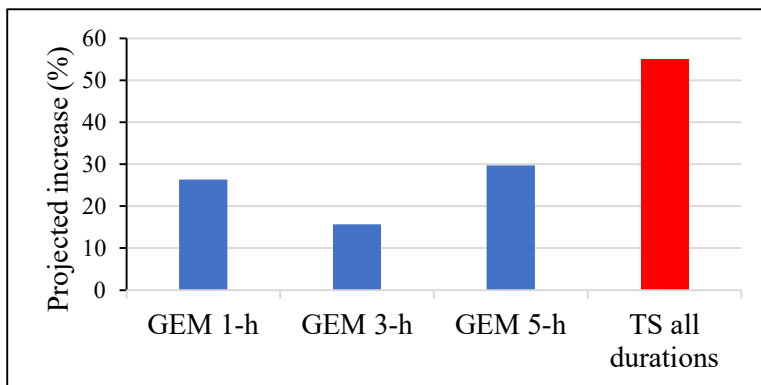


Figure 4.1 Projected changes to 100-year 1-, 3-, and 5-h precipitation using GEM and TS.

4.2 Preliminary exploration of added value using sub-km scale climate modelling

The climate model simulations considered in this study were performed at 4 km resolution. Running climate models at this resolution requires enormous computational resources while having the benefit that finer scale processes, including convection, are better resolved compared to coarser resolution models. Nonetheless, only around 24 grid cells of the GEM_ERA5 simulation

cover the study area. Using sub-km resolution climate simulations could be useful in capturing precipitation patterns in much greater detail. The added value of fine resolution is demonstrated through a preliminary simulation modelling the precipitation event on July 1, 2017, considered in Chapter 3. According to Fig. 4.2, GEM at 100 m resolution (GEM100_ERA5) better captures the peak and timing of precipitation compared to GEM simulation at 4 km (GEM4_ERA5).

Figure 4.3 shows the total precipitation over the study area based on GEM_ERA5 and GEM100_ERA5 for the event. Precipitation patterns are similar in both simulations, where total rainfall is generally higher in the southern parts. Nonetheless, coarser resolution in GEM_ERA5 has led to deficiencies in capturing a smooth pattern, while GEM100_ERA5 shows integrity in the simulated precipitation patterns. Moreover, GEM100_ERA5 show higher precipitation in most of the study site, especially in the northern and southern regions.

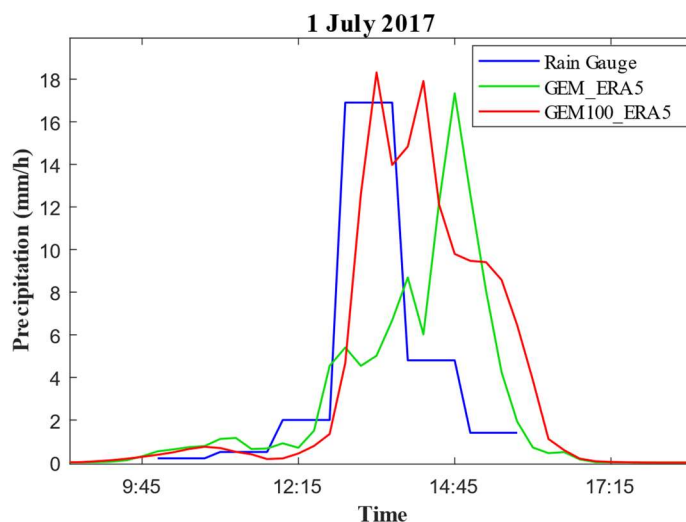


Figure 4.2 2017 July 1 event precipitation from GEM-ERA5 and GEM100-ERA5 simulations.

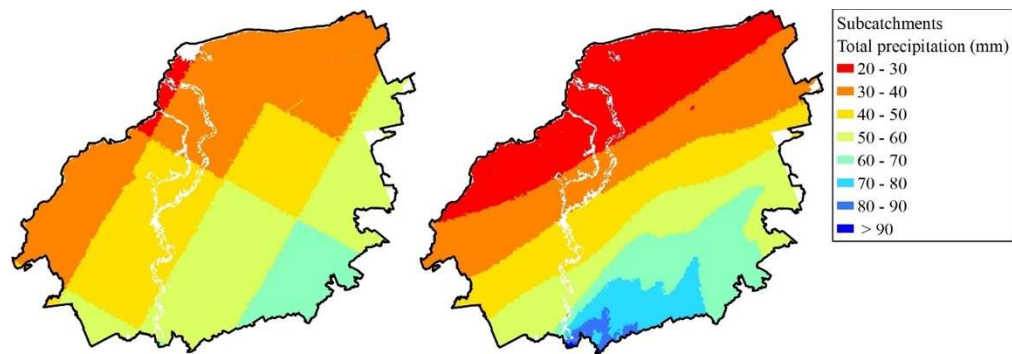


Figure 4.3 Total precipitation associated with the July 1, 2017 event from GEM_ERA5 (left) and GEM100_ERA5 (right) simulations.

It should be noted that such improvements are not achievable at no cost. Super-resolutions, like 100m, could be exceedingly costly in terms of computational time and resources. Hybrid methods, such as integrating machine learning methods with GEM model outputs, can also be investigated.

Employing higher resolution rainfall is particularly important in simulating flood depth over road links where the amount of rainfall received by each link may differ by employing sub-km resolutions. PFF simulations performed for the July 1, 2017 event using precipitation data from GEM_ERA5 and GEM100_ERA5 simulations show that max flood depth results have higher magnitudes in the southern regions for the latter than the former, implying the underestimation of precipitation using GEM_ERA5 in those areas compared to GEM100_ERA5 (Fig. 4.4), which is in accordance with the precipitation patterns shown in Fig 4.3. Moreover, several road segments receive different volumes of rainfall in the two simulations. These findings show how increasing the climate model resolution could impact the simulated flood depth on road links.

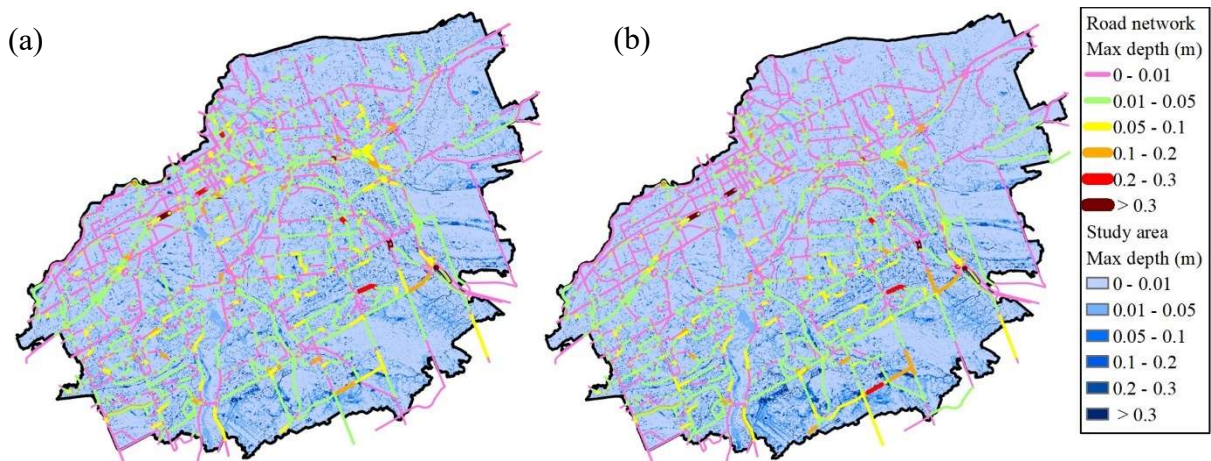


Figure 4.4 Max flood depth simulated using rainfall data from (a) GEM_ERA5, (b) GEM100_ERA5.

At the time of writing this thesis, it is not possible to undertake climate change simulations at 100 m resolution. It is expected that with continuous advances happening on the HPC front, this may become possible in the near future. Albeit these improvements that can be made in the future, this study sheds light on climate-traffic interactions for the study region.

CHAPTER 5 - CONCLUSIONS AND RECOMMENDATIONS

Pluvial flash floods can cause significant disruption to road networks. This is particularly crucial in urban settings due to the fact that a considerable proportion of surfaces are impermeable. Such impacts are projected to increase due to further urbanization and climate change which can result in more frequent extreme short-duration rainfall events.

Through the integration of ultra high resolution (4 km) GEM regional climate model simulations, inundation modelling with PCSWMM, and exposure analysis based on a GIS-based transport demand modelling, this study examines flash flood-traffic interactions for current (1991-2010) and future (2081-2100) climates for Ottawa, the capital city of Canada. Short-duration (i.e., 1-h, 3-h, and 5-h) precipitation events with 100-year return levels are taken into consideration where projected changes to the return levels of precipitation are estimated using two approaches: in the first approach, projected changes are obtained directly from the RCM simulation, whereas in the second approach, these are obtained using temperature scaling (TS). In addition to the qualitative validation of the hydrodynamic model-simulated flash flood depths for past flooding, quantitative validation of the RCM-simulated precipitation characteristics, i.e. intensity-duration relations for selected return levels and their spatial variability, against observations, confirms the suitability of the selected models for analyzing flash flood-related traffic disruptions.

Results show travel delays for the 100-year return levels of 1-h, 3-h, and 5-h events in the 48,000 to 55,000 range in the current climate, depending on the approach implemented. These delays are projected to increase in the future climate associated with projected increases in the considered return levels of precipitation and related flood depths. The projected increases to the total length of the blocked roads of the network, i.e. road links with water depths above 30 cm, are in the 24

to 36 km range. This, combined with significant increases in the floodwater depth for unblocked road links leading to significant speed reductions, augments traffic delays in future climate.

The two approaches considered in this study, namely GEM-based and TS-based, yield similar travel delays with slightly higher values using the former. The validity of the temperature scaling relation for all regions of Canada was not part of this research, but is worth exploring in future studies. For instance, Oh and Sushama (2020) in their study of short-duration precipitation extremes demonstrated significant differences in the precipitation-temperature relation across Canada. The GEM-based approach, being based on the physically-based climate model simulated precipitation, is devoid of such issues; the ultra-high resolution enables to capture high-intensity short-duration precipitation realistically, which is critical for studies such as the one addressed in this thesis.

While this study provides useful insight into the pluvial flash flood-traffic interactions, future studies/improvements that can further enhance the robustness of the results presented in this study are discussed below.

In order to assess the impact of climate change, this study considered RCP 8.5, which is business-as-usual scenario assuming no measures to curb greenhouse gas emissions. It should be noted that none of the RCP scenarios are more probable, and a more comprehensive analysis of future traffic-climate interactions should consider other RCP scenarios to quantify greenhouse gas emissions scenario uncertainties.

Climate models and driving data are other sources of uncertainties. In this study, GEM and CanESM2 are used as the climate model and the driving data, respectively. Multi-model ensembles

of RCM-driving GCM pairs are recommended to quantify these uncertainties; however, such efforts entail substantial computational resources.

In order to reduce computational costs, only the travel demands of the eight inner wards, constituting the study area, are considered in this study. Because the considered wards account for approximately 20% of the total traffic load reported in the Ottawa origin-destination matrix, traffic demands on the road links underestimate the actual traffic. This leads to lower total person hour and inaccurate trip paths as traffic speed is a function of flow on the road links. However, this will not translate into 80% underestimation in traffic loads, as traffic from external wards could include external trips, not passing the study region. In a more robust approach, one needs to account for all wards and travel demands.

This study assumes no changes to travel demand from the current to the future and this can be considered in future studies to further improve the realism. Moreover, the transport network is considered to be static. This may result in inaccuracies in terms of the modelled network and available paths between origins and destinations. A comprehensive four-step model could be performed to evaluate future traffic demands. Such modelling considers future demographic, economic, social, land use, and similar trends and generates future travel demands, which are then distributed between origins and destinations and split based on various modes of traffic.

This study employed ultra-high resolution (4km) RCM simulation. Climate modelling at sub-km scales could significantly improve the simulated precipitation spatial patterns and accuracy. However, this increase in the resolution entails substantial increases in the required computing resources and time.

The information provided in this research is crucial in guiding the development of adaptation measures to increase resilience in the transportation network. Critical road links based on flood water depth and traffic exposure can be prioritized to implement adaptation strategies, which could include hard engineering practices such as improving the drainage network capacity and increasing road elevation or nature-based solutions.

The methodology/framework developed here is transferable to any other urban region, subject to the availability of traffic data and ultra-high-resolution climate change information.

REFERENCES

- Agarwal, M., Maze, T. H., & Souleyrette, R. (2005, August). Impacts of weather on urban freeway traffic flow characteristics and facility capacity. In Proceedings of the 2005 mid-continent transportation research symposium (pp. 18-19).
- Ahiablame, L., & Shakya, R. (2016). Modelling flood reduction effects of low impact development at a watershed scale. *Journal of environmental management*, 171, 81-91.
- Akhter, M. S., & Hewa, G. A. (2016). The use of PCSWMM for assessing the impacts of land use changes on hydrological responses and performance of WSUD in managing the impacts at Myponga catchment, South Australia. *Water*, 8(11), 511.
- Andrey, J., Mills, B., Leahy, M., & Suggett, J. (2003). Weather as a chronic hazard for road transportation in Canadian cities. *Natural hazards*, 28(2), 319-343.
- Arkell, B. P., & Darch, G. J. C. (2006, December). Impact of climate change on London's transport network. In Proceedings of The Institution of Civil Engineers-Municipal Engineer (Vol. 159, No. 4, pp. 231-237). Thomas Telford Ltd.
- Arora, V. K., Scinocca, J. F., Boer, G. J., Christian, J. R., Denman, K. L., Flato, G. M., ... & Merryfield, W. J. (2011). Carbon emission limits required to satisfy future representative concentration pathways of greenhouse gases. *Geophysical Research Letters*, 38(5).
- Bamford, T., Balmforth, D., Digman, C., Waller, S., & Hunter, N. (2008). Modelling flood risk assessment, an evaluation of different methods. In WaPUG autumn conference.
- Barredo, J. I. (2009). Normalised flood losses in Europe: 1970–2006. *Natural hazards and earth system sciences*, 9(1), 97-104.
- Brown, S., & Dawson, R. (2016). Building network-level resilience to resource disruption from flooding: Case studies from the Shetland Islands and Hurricane Sandy. In E3S Web of Conferences (Vol. 7, p. 04008). EDP Sciences.
- TRANS report (2013), http://www.ncr-trans-rcn.ca/wp-content/uploads/2013/03/1995_TRANS_Model_Calibration.pdf
- Chapleau, R., & Morency, C. (2005). Dynamic spatial analysis of urban travel survey data using GIS. In 25th Annual ESRI International User Conference, San Diego, California (pp. 1-14).
- Chen, X. (2008). Microsimulation of hurricane evacuation strategies of Galveston Island. *The Professional Geographer*, 60(2), 160-173.
- Chung, E., Ohtani, O., Warita, H., Kuwahara, M., & Morita, H. (2005, September). Effect of rain on travel demand and traffic accidents. In Proceedings. 2005 IEEE Intelligent Transportation Systems, 2005. (pp. 1080-1083). IEEE.
- Côté, J., Gravel, S., Méthot, A., Patoine, A., Roch, M., & Staniforth, A. (1998). The operational CMC–MRB global environmental multiscale (GEM) model. Part I: Design considerations and formulation. *Monthly Weather Review*, 126(6), 1373-1395.

- Coulombe, A., Martel, J. L., Poulin, A., Glaus, M., Audet, G., & Girard, S. (2022). Assessment of Adaptation Solutions to Floods with PCSWMM and a Multicriteria Analysis for a Very Small Watershed. In Canadian Society of Civil Engineering Annual Conference (pp. 321-334). Springer, Singapore.
- CSA (Canadian Standards Association). (2012). Technical guide-development, interpretation and use of rainfall intensity-duration-frequency (IDF) information: Guideline for Canadian water resources practitioners.
- Dalziell, E., & Nicholson, A. (2001). Risk and impact of natural hazards on a road network. *Journal of transportation engineering*, 127(2), 159-166.
- de Dios Ortúzar, J., & Willumsen, L. G. (2011). *Modelling transport*. John Wiley & sons.
- Department for Transport. (2014). *Transport Resilience Review: A review of the resilience of the transport network to extreme weather events*.
- Diro, G. T., & Sushama, L. (2020). Contribution of snow cover decline to projected warming over North America. *Geophysical Research Letters*, 47(1), e2019GL084414.
- Dutta, D., Herath, S., & Musiake, K. (2003). A mathematical model for flood loss estimation. *Journal of hydrology*, 277(1-2), 24-49.
- Eisenberg, D. (2004). The mixed effects of precipitation on traffic crashes. *Accident analysis & prevention*, 36(4), 637-647.
- Fowler, H. J., & Wilby, R. L. (2010). Detecting changes in seasonal precipitation extremes using regional climate model projections: Implications for managing fluvial flood risk. *Water Resources Research*, 46(3).
- Fu, G., Dawson, R., Khoury, M., & Bullock, S. (2014). Interdependent networks: vulnerability analysis and strategies to limit cascading failure. *The European Physical Journal B*, 87(7), 1-10.
- Giorgi, F. (2019). Thirty years of regional climate modelling: where are we and where are we going next?. *Journal of Geophysical Research: Atmospheres*, 124(11), 5696-5723.
- Gooré Bi, E., Monette, F., Gachon, P., Gasperi, J., & Perrodin, Y. (2015). Quantitative and qualitative assessment of the impact of climate change on a combined sewer overflow and its receiving water body. *Environmental Science and Pollution Research*, 22(15), 11905-11921.
- Hammond, M. J., Chen, A. S., Djordjević, S., Butler, D., & Mark, O. (2015). Urban flood impact assessment: A state-of-the-art review. *Urban Water Journal*, 12(1), 14-29.
- Held, I. M., & Soden, B. J. (2006). Robust responses of the hydrological cycle to global warming. *Journal of climate*, 19(21), 5686-5699.
- Hersbach, H., Bell, B., Berrisford, P., Hirahara, S., Horányi, A., Muñoz-Sabater, J., ... & Thépaut, J. N. (2020). The ERA5 global reanalysis. *Quarterly Journal of the Royal Meteorological Society*, 146(730), 1999-2049.

- Hooper, E., Chapman, L., & Quinn, A. (2014). The impact of precipitation on speed–flow relationships along a UK motorway corridor. *Theoretical and applied climatology*, 117(1), 303-316.
- Houghton, J., Reiners, J., & Lim, C. (2009). Intelligent transport: How cities can improve mobility. IBM Institute for Business Value, 1-6.
- Ilägrstrand, T. (1970). What about people in regional science. *regional science association*, 24.
- Infrastructure, C. (2016). Canadian infrastructure report card-informing the future.
- IPCC, 2013. *Climate Change 2013: The Physical Science Basis*. Cambridge University Press, Cambridge.
- James, R., Finney, K., Randall, M., & Heralall, M. Development of a Real Time Flood Forecasting System-Toronto, Canada.
- Jaroszweski, D., Chapman, L., & Petts, J. (2010). Assessing the potential impact of climate change on transportation: the need for an interdisciplinary approach. *Journal of Transport Geography*, 18(2), 331-335.
- Jonkman, S. N., & Kelman, I. (2005). An analysis of the causes and circumstances of flood disaster deaths. *Disasters*, 29(1), 75-97.
- Jonkman, S. N., Bočkarjova, M., Kok, M., & Bernardini, P. (2008a). Integrated hydrodynamic and economic modelling of flood damage in the Netherlands. *Ecological economics*, 66(1), 77-90.
- Jonkman, S. N., Vrijling, J. K., & Vrouwenvelder, A. C. W. M. (2008b). Methods for the estimation of loss of life due to floods: a literature review and a proposal for a new method. *Natural Hazards*, 46(3), 353-389.
- Keifer, C. J., & Chu, H. H. (1957). Synthetic storm pattern for drainage design. *Journal of the hydraulics division*, 83(4), 1332-1.
- Kellermann, P., Schönberger, C., & Thielen, A. H. (2016). Large-scale application of the flood damage model RAILway Infrastructure Loss (RAIL). *Natural Hazards and Earth System Sciences*, 16(11), 2357-2371.
- Kendon, E. J., Roberts, N. M., Senior, C. A., & Roberts, M. J. (2012). Realism of rainfall in a very high-resolution regional climate model. *Journal of Climate*, 25(17), 5791-5806.
- Koetse, M. J., & Rietveld, P. (2009). The impact of climate change and weather on transport: An overview of empirical findings. *Transportation Research Part D: Transport and Environment*, 14(3), 205-221.
- Kyte, M., Khatib, Z., Shannon, P., & Kitchener, F. (2000, June). Effect of environmental factors on free-flow speed. In *Fourth International Symposium on Highway Capacity* (pp. 108-119).
- Leandro, J., Chen, A. S., Djordjević, S., & Savić, D. A. (2009). Comparison of 1D/1D and 1D/2D coupled (sewer/surface) hydraulic models for urban flood simulation. *Journal of hydraulic engineering*, 135(6), 495-504.

- Li, M., Huang, Q., Wang, L., Yin, J., & Wang, J. (2018). Modelling the traffic disruption caused by pluvial flash flood on intra-urban road network. *Transactions in GIS*, 22(1), 311-322.
- Manchikatla, S. K., & Umamahesh, N. V. (2022). Simulation of flood hazard, prioritization of critical sub-catchments, and resilience study in an urban setting using PCSWMM: a case study. *Water Policy*, 24(8), 1247-1268.
- Mao, L. Z., Zhu, H. G., & Duan, L. R. (2012). The social cost of traffic congestion and countermeasures in Beijing. In *Sustainable Transportation Systems: Plan, Design, Build, Manage, and Maintain* (pp. 68-76).
- Mark, O., Weesakul, S., Apirumanekul, C., Aroonnet, S. B., & Djordjević, S. (2004). Potential and limitations of 1D modelling of urban flooding. *Journal of Hydrology*, 299(3-4), 284-299.
- Mitchell, J. K. (2003). European river floods in a changing world. *Risk Analysis: An International Journal*, 23(3), 567-574.
- Mote, T. L., Lacke, M. C., & Shepherd, J. M. (2007). Radar signatures of the urban effect on precipitation distribution: A case study for Atlanta, Georgia. *Geophysical Research Letters*, 34(20).
- Oh, S. G., & Sushama, L. (2020). Short-duration precipitation extremes over Canada in a warmer climate. *Climate Dynamics*, 54(3), 2493-2509.
- Palmer, T. (2014). Climate forecasting: Build high-resolution global climate models. *Nature*, 515(7527), 338-339.
- Park, B. B., & Kwak, J. (2011). Calibration and validation of TRANSIMS microsimulator for an urban arterial network. *KSCE Journal of Civil Engineering*, 15(6), 1091-1100.
- Peng, Z., Jinyan, K., Wenbin, P., Xin, Z., & Yuanbin, C. (2019). Effects of Low-Impact Development on Urban Rainfall Runoff under Different Rainfall Characteristics. *Polish Journal of Environmental Studies*, 28(2).
- Penning-Rowsell, E., Priest, S., Parker, D., Morris, J., Tunstall, S., Viavattene, C., ... & Owen, D. (2014). *Flood and coastal erosion risk management: a manual for economic appraisal*. Routledge.
- Pregolato, M., Ford, A., & Dawson, R. (2016). Disruption and adaptation of urban transport networks from flooding. In *E3s Web of conferences* (Vol. 7, p. 07006). EDP Sciences.
- Pregolato, M., Ford, A., Glenis, V., Wilkinson, S., & Dawson, R. (2017). Impact of climate change on disruption to urban transport networks from pluvial flooding. *Journal of Infrastructure Systems*, 23(4), 04017015.
- Prein, A. F., Gobiet, A., Suklitsch, M., Truhetz, H., Awan, N. K., Keuler, K., and Georgievski, G. (2013). Added value of convection permitting seasonal simulations. *Climate Dynamics*, 41(9-10), 2655-2677.
- Prein, A. F., Holland, G. J., Rasmussen, R. M., Done, J., Ikeda, K., Clark, M. P., and Liu, C. H. (2013). Importance of regional climate model grid spacing for the simulation of heavy precipitation in the Colorado headwaters. *Journal of climate*, 26(13), 4848-4857.

- Prein, A. F., Langhans, W., Fosser, G., Ferrone, A., Ban, N., Goergen, K., ... and Leung, R. (2015). A review on regional convection-permitting climate modelling: Demonstrations, prospects, and challenges. *Reviews of geophysics*, 53(2), 323-361.
- Rummukainen, M. (2010). State-of-the-art with regional climate models. *Wiley Interdisciplinary Reviews: Climate Change*, 1(1), 82-96.
- Salathé, E. P., & Mauger, G. (2018). Climate Change, Heavy Precipitation and Flood Risk in the Western United States. In *Climate Change and Its Impacts* (pp. 109-127). Springer, Cham.
- Scawthorn, C., Flores, P., Blais, N., Seligson, H., Tate, E., Chang, S., ... & Lawrence, M. (2006). HAZUS-MH flood loss estimation methodology. II. Damage and loss assessment. *Natural Hazards Review*, 7(2), 72-81.
- Shepherd, J. M., Pierce, H., & Negri, A. J. (2002). Rainfall modification by major urban areas: Observations from spaceborne rain radar on the TRMM satellite. *Journal of applied meteorology*, 41(7), 689-701.
- Shu, C., Xia, J., Falconer, R. A., & Lin, B. (2011). Incipient velocity for partially submerged vehicles in floodwaters. *Journal of hydraulic research*, 49(6), 709-717.
- Spekkers, M. H., Ten Veldhuis, J. A. E., & Clemens, F. H. L. R. (2011). Collecting data for quantitative research on pluvial flooding. In *12th International Conference on Urban Drainage*, Porto Alegre, Brazil, 11-15 September 2011. IWA-International Water Association.
- Su, B., Huang, H., & Li, Y. (2016). Integrated simulation method for waterlogging and traffic congestion under urban rainstorms. *Natural Hazards*, 81(1), 23-40.
- Sushama, L., B. Teufel, J. Atrill, A. Faki, V. Poitras, L. Duarte. (2021). Engineering climate simulations and thresholds for Nunavut. Transport Canada Technical Report. P119.
- Teufel, B., & Sushama, L. (2022). High-resolution modelling of climatic hazards relevant for Canada's northern transportation sector. *Climate Dynamics*, 1-17. Tingsanchali, T. (2012). Urban flood disaster management. *Procedia engineering*, 32, 25-37.
- Thornton, P. E., Thornton, M. M., Mayer, B. W., Wei, Y., Devarakonda, R., Vose, R. S., & Cook, R. B. (2016). Daymet: daily surface weather data on a 1-km grid for North America, version 3. ORNL DAAC, Oak Ridge, Tennessee, USA. USDA-NASS, 2019. 2017 Census of Agriculture, Summary and State Data, Geographic Area Series, Part 51, AC-17-A-51.
- Trenberth, K. E. (2011). Changes in precipitation with climate change. *Climate research*, 47(1-2), 123-138.
- Tsapakis, I., Cheng, T., & Bolbol, A. (2013). Impact of weather conditions on macroscopic urban travel times. *Journal of Transport Geography*, 28, 204-211.
- Verseghy DL (2011) CLASS—the canadian land surface scheme (version 3.5), technical documentation (version 1). Climate Research Division, Science and Technology Branch, Environment Canada

- Versini, P. A., Gaume, E., & Andrieu, H. (2010). Application of a distributed hydrological model to the design of a road inundation warning system for flash flood prone areas. *Natural Hazards and Earth System Sciences*, 10(4), 805-817.
- Walker, J. L. (2005). Making household microsimulation of travel and activities accessible to planners. *Transportation research record*, 1931(1), 38-48.
- Warner, M. D., Mass, C. F., & Salathé, E. P. (2012). Wintertime extreme precipitation events along the Pacific Northwest coast: Climatology and synoptic evolution. *Monthly Weather Review*, 140(7), 2021-2043.
- Williams, H. C. (1977). On the formation of travel demand models and economic evaluation measures of user benefit. *Environment and planning A*, 9(3), 285-344.
- Xia, J., Falconer, R. A., Xiao, X., & Wang, Y. (2014). Criterion of vehicle stability in floodwaters based on theoretical and experimental studies. *Natural hazards*, 70(2), 1619-1630.
- Xia, J., Teo, F. Y., Lin, B., & Falconer, R. A. (2011). Formula of incipient velocity for flooded vehicles. *Natural Hazards*, 58(1), 1-14.
- Yin, J., Yu, D., Yin, Z., Liu, M., & He, Q. (2016). Evaluating the impact and risk of pluvial flash flood on intra-urban road network: A case study in the city center of Shanghai, China. *Journal of hydrology*, 537, 138-145.
- Zhong, M., Shan, R., Du, D., & Lu, C. (2015). A comparative analysis of traditional four-step and activity-based travel demand modelling: a case study of Tampa, Florida. *Transportation Planning and Technology*, 38(5), 517-533.
- Zio, E. (2016). Critical infrastructures vulnerability and risk analysis. *European Journal for Security Research*, 1(2), 97-114.